AD-A048 849 JOHNS HOPKINS UNIV LAUREL MD APPLIED PHYSICS LAB F/G 16/4
EXPERIMENTAL INVESTIGATIONS AT MACH 0.8 OF THE STABILITY AND CO--ETC(U)
AUG 77 E F LUCERO N00017-72-C-4401
UNCLASSIFIED APL/JHU/TG-1312 NL

| OF |
AD
A048849

END
DATE
FILMED
2-78
DDC

APL/JHU
TG 1312
AUGUST 1977
Copy No. 1

Technical Memorandum

EXPERIMENTAL INVESTIGATIONS AT MACH 0.8 OF THE STABILITY AND CONTROL CHARACTERISTICS OF MISSILE CONFIGURATIONS WITH WRAPAROUND SURFACES

By E. F. LUCERO

THE JOHNS HOPKINS UNIVERSITY ■ APPLIED PHYSICS LABORATORY

Unclassified

SECURITY CLASSIFICATION OF THIS PAGE

PLEASE FOLD BACK IF NOT NEEDED FOR BIBLIOGRAPHIC PURPOSES

REPORT DOCUMENTATION PAGE

1. REPORT NUMBER: APL/JHU/TG-1312	2. GOVT ACCESSION NO.
3. RECIPIENT'S CATALOG NUMBER	
4. TITLE (*and Subtitle*): EXPERIMENTAL INVESTIGATIONS AT MACH 0.8 OF THE STABILITY AND CONTROL CHARACTERISTICS OF MISSILE CONFIGURATIONS WITH WRAPAROUND SURFACES.	5. TYPE OF REPORT & PERIOD COVERED: Technical Memorandum
	6. PERFORMING ORG. REPORT NUMBER: TG 1312
7. AUTHOR(s): E. F. Lucero	8. CONTRACT OR GRANT NUMBER(s): N00017-72-C-4401
9. PERFORMING ORGANIZATION NAME & ADDRESS: The Johns Hopkins University Applied Physics Laboratory, Johns Hopkins Rd., Laurel, MD 20810	10. PROGRAM ELEMENT, PROJECT, TASK AREA & WORK UNIT NUMBERS: A31
11. CONTROLLING OFFICE NAME & ADDRESS: Naval Sea Systems Command, SEA-0351, Washington, DC 20362	12. REPORT DATE: August 1977
	13. NUMBER OF PAGES: 88
14. MONITORING AGENCY NAME & ADDRESS: Naval Plant Representative Office, Johns Hopkins Rd., Laurel, MD 20810	15. SECURITY CLASS. (*of this report*): Unclassified
	15a. DECLASSIFICATION/DOWNGRADING SCHEDULE

16. DISTRIBUTION STATEMENT (*of this Report*)

Approved for public release; distribution unlimited.

17. DISTRIBUTION STATEMENT (*of the abstract entered in Block 20, if different from Report*)

18. SUPPLEMENTARY NOTES

19. KEY WORDS (*Continue on reverse side if necessary and identify by block number*)

bank-to-turn missiles
missile aerodynamics
stability and control
transonic aerodynamics
wraparound surfaces

20. ABSTRACT (*Continue on reverse side if necessary and identify by block number*)

The aerodynamic feasibility of using wraparound lifting, stabilizing, and controlling surfaces on tube-launched bank-to-turn missile configurations is established by wind tunnel tests at high subsonic speeds. Test results show that the stability and control characteristics of a wraparound-surface configuration are as good or better than those of an equivalent planar-surface configuration. Predictions based on planar surfaces agree well with test results when surface-to-surface interference is not present. An improved prediction method for tail efficiency of wraparound-surface configurations is shown. Several configurational design preferences are indicated by the test results, including high wings with concave side windward, horizontal tails mounted with their concave side windward when in the undeflected position, and a windward directional stabilizer.

DD FORM 1 JAN 73 1473

031 650

Unclassified

SECURITY CLASSIFICATION OF THIS PAGE

APL/JHU
TG 1312
AUGUST 1977

Technical Memorandum

EXPERIMENTAL INVESTIGATIONS AT MACH 0.8 OF THE STABILITY AND CONTROL CHARACTERISTICS OF MISSILE CONFIGURATIONS WITH WRAPAROUND SURFACES

By E. F. LUCERO

THE JOHNS HOPKINS UNIVERSITY ■ APPLIED PHYSICS LABORATORY
Johns Hopkins Road, Laurel, Maryland 20810
Operating under Contract N00017-72-C-4401 with the Department of the Navy

THE JOHNS HOPKINS UNIVERSITY
APPLIED PHYSICS LABORATORY
LAUREL MARYLAND

ABSTRACT

The aerodynamic feasibility of using wraparound lifting, stabilizing, and controlling surfaces on tube-launched bank-to-turn missile configurations is established by wind tunnel tests at high subsonic speeds. Test results show that the stability and control characteristics of a wraparound-surface configuration are as good or better than those of an equivalent planar-surface configuration. Predictions based on planar surfaces agree well with test results when surface-to-surface interference is not present. An improved prediction method for tail efficiency of wraparound-surface configurations is shown. Several configurational design preferences are indicated by the test results, including high wings with concave side windward, horizontal tails mounted with their concave side windward when in the undeflected position, and a windward directional stabilizer.

SUMMARY

The feasibility of using wraparound lifting, stabilizing, and control surfaces on tube-launched, bank-to-turn missile configurations was investigated in a wind tunnel, mostly at Mach 0.8. Longitudinal and lateral stability and control data were obtained on configurations having monoplane wings that wrap around the missile body when it is in the stored position, a wraparound horizontal tail, and planar vertical tail. The analysis of the test results is presented in this report. Comparisons of these data with data obtained for a similar configuration having planar suffaces and with the predictive methods derived for planar surfaces are also shown.

In general, the use of wraparound surfaces for lift, stability, and control of bank-to-turn missile configurations appears feasible; the longitudinal, directional, and roll stability and control characteristics of the wraparound-surface configuration are as good or better than those of the equivalent planar-surface configuration. No unusual aerodynamic behavior affecting stability or control was exhibited by the configurations.

The lift of wraparound surfaces can be reasonably predicted either from theory or from empirical methods derived for planar surfaces, provided that the projected planforms are the same and that surface-to-surface interference is not significant. An improved prediction method for tail efficiency of wraparound surfaces is shown. It uses an empirically derived tail height parameter used in existing downwash formulations in place of the height used for planar surfaces. Control-surface effectiveness for body-wing-tail configurations can be predicted well using empirical correlations provided that body-tail data are available; otherwise theoretical methods provide a conservative prediction that is acceptable for preliminary design. Empirical methods are recommended for estimating body-alone longitudinal stability; cross-flow theory provides a good prediction of the body-alone normal force coefficient, but it predicts the center-of-pressure to be too far forward on the body.

On configurational design, high-wing (concave side windward) configurations are aerodynamically preferable to low-wing (convex side windward) configurations; horizontal tails mounted with their concave side windward (in the undeflected position) are preferred; a windward vertical tail is more effective in providing directional

stability than a leeward vertical tail; a wraparound vertical tail is more effective in providing directional stability than a planar vertical tail. From all observations on the aerodynamic effectiveness of wraparound surfaces, a configuration having all wraparound surfaces appears to be aerodynamically feasible.

CONTENTS

ILLUSTRATIONS

TABLES

1. INTRODUCTION

In most Navy missile systems, a major constraint on the design of the aerodynamic configuration results from the choice of the launching system. Recent interest in tube-type launching systems leads naturally to consideration of configurations with foldable or wraparound lifting surfaces that fit compactly into such launchers and that also provide satisfactory aerodynamic performance with the surfaces deployed for flight. In the stowed position these surfaces would be folded so as to fit within a circular cylinder defined by the maximum diameter of the missile body.

The present study has concentrated on the use of surfaces that wrap around the missile in its stowed position so as to maximize the volume available in the missile. Most previous interest in wraparound surfaces has been in their application as stabilizing fins on bombs and projectiles (Refs. 1 through 7). The specific application prompting the present study would be in a missile using a bank-to-turn control system and cruising subsonically.

Ref. 1. H. J. Gauzza, "Static Stability Test of Tangent and Wrap-Around Fin Configurations at Supersonic Speeds," NAVORD Report 3743, 17 January 1955.

Ref. 2. R. Franklin Wells, "Investigation of the Aerodynamic Characteristics of a Model of a Rocket Missile with Several Arrangements of Folding Fins at Mach Numbers of 1.75, 2.15, 2.48, and 2.87," NASA TMX-234, April 1960.

Ref. 3. H. A. Featherstone, "The Aerodynamic Characteristics of Curved Tail Fins," General Dynamics/Pomona GDC-ERR-PO-019, September 1960.

Ref. 4. F. J. Regan and V. L. Schermerhorn, "Supersonic Magnus Measurements of the 10-Caliber Army-Navy Spinner Projectile with Wrap-Around Fins," NOL TR 70-211, 1 October 1970.

Ref. 5. Proceedings of the Ninth Meeting of the Exterior Ballistics Panel 0-7, Vol. II, Session I, Weapon Aerodynamics, DREV M-2184172, September to October 1971 (see Bibliography for pertinent papers).

Ref. 6. J. C. Craft and J. Skorupski, "Static Aerodynamic Stability Characteristics of Munitions Designs at Transonic Mach Numbers," USAMC Tech Report RD-73-3, February 1973.

Ref. 7. C. W. Dahlke and J. C. Craft, "Aerodynamic Characteristics of Wrap Around Fins Mounted on Bodies of Revolution, and Their Influence on Missile Static Stability at Mach Numbers from 0.3 to 1.3," USAMC RD-TM-72-1, Vol. I, March 1972, Vol. II, April 1972.

OBJECTIVE OF PROGRAM

The objective of this exploratory development program was to assess the aerodynamic feasibility of a configuration using wraparound wings and wraparound or foldable stabilizing and control surfaces. The scope of the study was limited to consideration of a missile that would operate at high subsonic speeds, using a bank-to-turn control system.

TECHNICAL APPROACH

The general approach used in carrying out the study involved the following phases:

1. Preliminary aerodynamic design of a missile configuration meant for cruising at high subsonic speeds using wraparound surfaces, and of a similar configuration using planar surfaces of the same projected planform;

2. Wind-tunnel testing of the longitudinal and lateral stability and control characteristics of the two configurations;

3. Comparison of the measured characteristics of the planar and warparound configurations. This comparison was used to ascertain whether predictions could be made of configurations using wraparound surfaces based on the characteristics of configurations using "equivalent" planar surfaces. If such a prediction scheme were possible, the large body of existing data on planar surfaces would be available for preliminary design of wraparound surfaces; and

4. Delineation of the aerodynamic advantages and disadvantages of the wraparound surfaces for the application being considered.

2. DESIGN AND SELECTION OF TEST CONFIGURATIONS

GENERAL DESIGN CONSIDERATIONS

Previous investigators of the aerodynamics of wraparound surfaces have established that, for a given projected planform and for essentially constant thickness profiles, the wraparound surfaces provide, at small angles of attack, about the same normal force and longitudinal stability as the planar surfaces (Refs. 4, 5, and 7). For this reason, in the absence of analytical methods for estimating the aerodynamics of wraparound surfaces and because of other considerations discussed in Ref. 8, theoretical and empirical methods developed for planar surfaces (e.g., Refs. 9 through 12), were used in this study for arriving at the design of the wraparound wings and tails. The surface planform and profile and the design Mach number were selected from considerations of lift-to-drag ratio and transonic performance (see Component Design Considerations discussed next). The body-wing-tail test configurations are described in Refs. 13 and 14 and shown schematically in Fig. 1.

Ref. 8. E. F. Lucero, "Proposal for Aerodynamic Investigation of Transonic Missile Configurations Incorporating Wrap-Around Lifting Surfaces, Part I: Aerodynamic Configuration Design," APL/JHU BBA-2-73-001, 2 April 1973

Ref. 9. F. W. Diederich, "A Planform Parameter for Correlating Certain Aerodynamic Characteristics of Swept Wings," NACA TN 2335, April 1951.

Ref. 10. W. C. Pitts, J. N. Nielsen, and G. E. Kaattari, "Lift and Center-of-Pressure of Wing-Body-Tail Combinations at Subsonic, Transonic, and Supersonic Speeds," NACA Report 1307, 1957.

Ref. 11. J. L. Decker, "Prediction of Downwash at Various Angles of Attack for Arbitrary Tail Locations," Aeronaut. Eng. Rev., Vol. 15, August 1956.

Ref. 12. "USAF Stability and Control DATCOM," McDonnell-Douglas Corp., Douglas Aircraft Division, under Contract to Air Force Flight Dynamics Laboratory, Wright-Patterson Air Force Base, Ohio, October 1960.

Ref. 13. E. F. Lucero, "Test Opeations Report, WASP Wind Tunnel Test No. HST 361-0 (August 7 - August 10, 1973)," APL/JHU BBA-2-73-005, 31 August 1973.

Ref. 14. E. F. Lucero, "Test Operations Report for WASP Controls Test GD/Convair HST 361-1 (August 21 - August 24, 1974)," APL/JHU BFD-1-74-022, 19 September 1974.

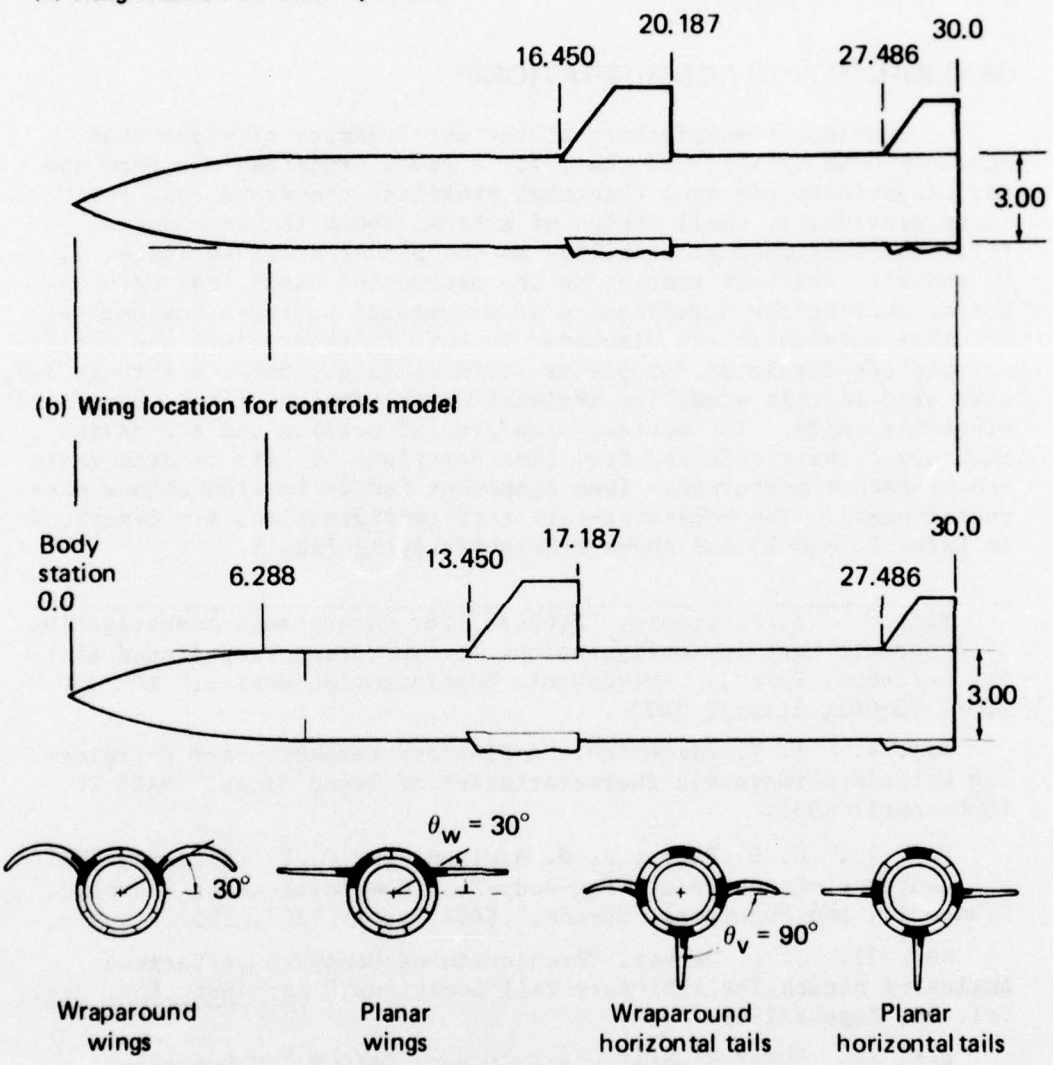

All dimensions are in inches

Fig. 1 Test Configurations

Specific factors leading to the final choice of the various components (i.e., body, wings, and tails) are discussed in the following paragraphs.

COMPONENT DESIGN CONSIDERATIONS

Body

Since drag investigation was not a primary objective, the choice of a configuration for the body was based primarily on considerations of fabrication costs and simplicity of model design. Thus, the use of existing models overrode the choice of an optimum body having a low-drag subsonic nose shape, a contoured section that accommodates the wings and tails when they are in their stowed positions, and a boattailed afterbody. The body selected for testing (Fig. 1) has a von Karman nose of fineness ratio 2.1, followed by a cylindrical body. The overall fineness ratio of 10 was selected on the basis of representative fineness ratios of existing tube-launched missiles (both U.S. and foreign) whose fineness ratios range from 6 to 13 (Ref. 15).

Wings

The geometric parameters considered in the design of the wing (Fig. 2) were span, profile, and planform.

The wingspan is limited by the requirement that it be wrapped around the body for tube stowage. To obtain the maximum span when the wings are unfolded (without having overlap when folded) the wing is located circumferentially on the body with its root chord elevated 30° above the horizontal plane of symmetry of the cylinder (Fig. 2).

A symmetrical profile was considered at the outset to minimize the testing required to obtain information on both high and low wing configurations and on concavity effects (concave and convex). High- and low-wing information is obtained by simply testing one configuration at both positive and negative angles of attack. This symmetrical profile also helps to avoid zero-shift problems in data interpretation. The profile was selected partly on the basis of its favorable drag divergence and on its stall

---

Ref. 15, "International Aerospace, 1972 Specification Tables" (Reprinted from Aviat. Week Space Technol.), 13 March 1972.

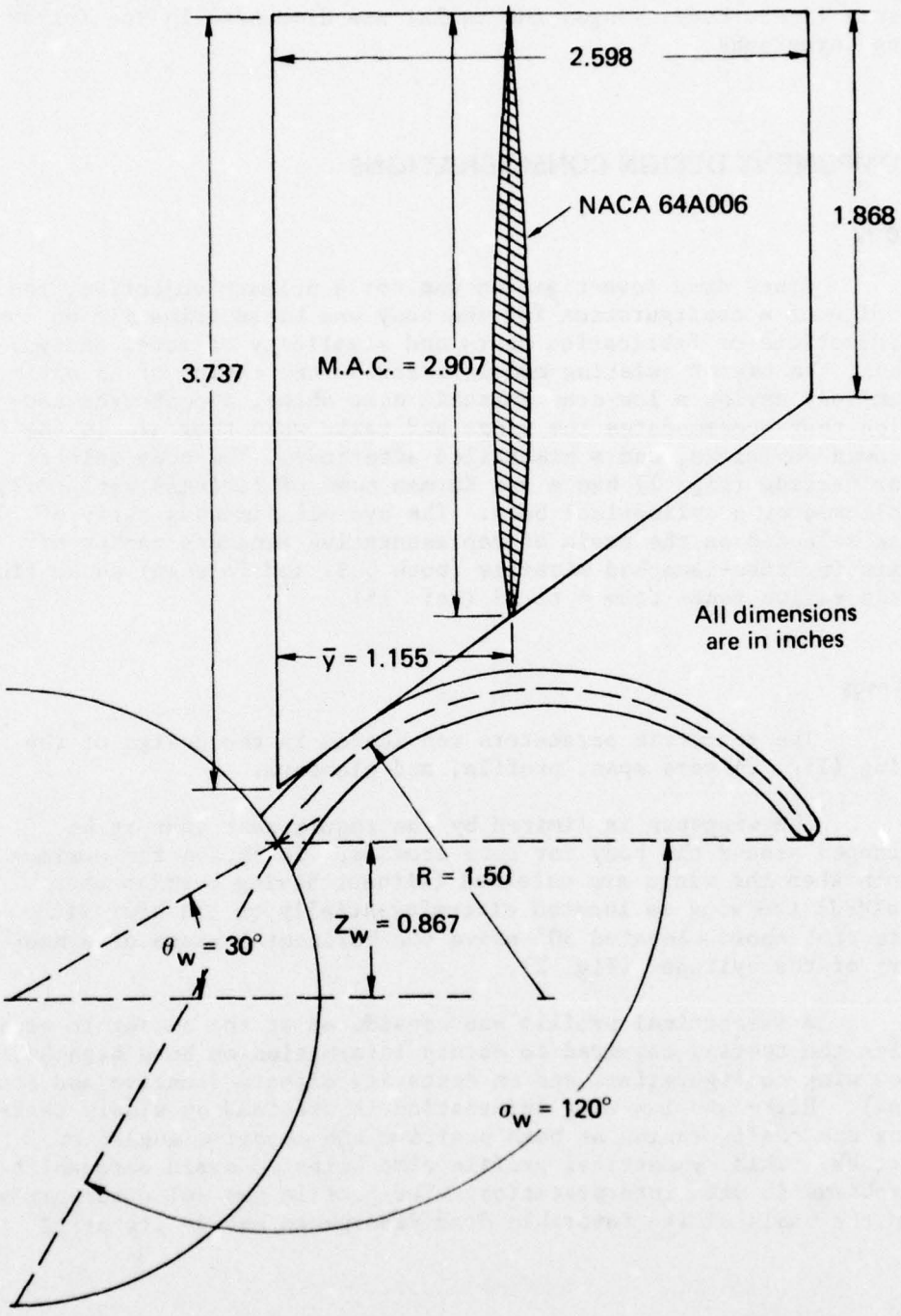

Fig. 2 Wraparound Wing Design

characteristics at angle of attack and at transonic speeds (Refs. 8, 16, and 17). An NACA 64A006 profile was selected, based on these transonic aerodynamic characteristics. The Mach number selected for the wing design was that estimated to be below the critical Mach number for the NACA 64A006 airfoil. The design Mach number is 0.8.

The primary considerations in planform design were (a) to obtain a combination of aspect ratio and area that optimizes the wing loading per degree of angle of attack, (b) to minimize losses in volume due to folding requirements, and (c) to maintain a high critical Mach number, which is dependent on sweep and profile (see Sections II.C and II.D of Ref. 8)*. The resulting wing planform is trapezoidal with a tip-to-root chord ratio of 1/2, has an exposed aspect ratio of 0.927, and is unswept at the trailing edge (Fig. 2), i.e., a clipped delta planform.

Horizontal Stabilizer (Control)

The horizontal stabilizer (control) (Fig. 3) was designed using basically the same considerations as those used in the wing design, but it was sized to provide neutral longitudinal stability at low angle of attack when the wing was located with its 1/4-chord point of the mean aerodynamic chord (M.A.C.) at $X/\ell_B = 0.60$ and when the center of gravity was at $X/\ell_B = 0.55$. (This center of gravity is typical of center-of-gravity locations of realistic missile configurations.) The horizontal stabilizer was mounted on the mid-plane of the cylinder, i.e., below the wing (Fig. 1), in order to reduce direct interference from the wing at positive angles of attack. The resulting planform of the horizontal stabilizer is similar to that of the wing but smaller (Fig. 3). The horizontal stabilizer has the NACA 64A006 profile.

---

*Mach number effects can also be minimized by "treating" the wing planform at the root chord and tip (e.g., Appendix D, of Ref. 18), but it was desirable in this study to keep the planform simple.

Ref. 16. B. N. Daley and R. S. Dick, "Effect of Thickness Camber and Thickness Distribution on Airfoil Characteristics at Mach Numbers up to 1.0," NACA TN 3607, March 1956.

Ref. 17. E. C. Allen, "Experimental Investigations of the Effects of Planform Taper on the Aerodynamic Characteristics of Symmetrical Unswept Wings of Varying Aspect Ratio," NACA RM A53 C19, 29 May 1953.

Ref. 18. E. F. Lucero and J. J. Pasierb, "Short Course on Current Transonic Flow Problems — Theories and Applications," APL/JHU BBA-0-74-003, 1 February 1974.

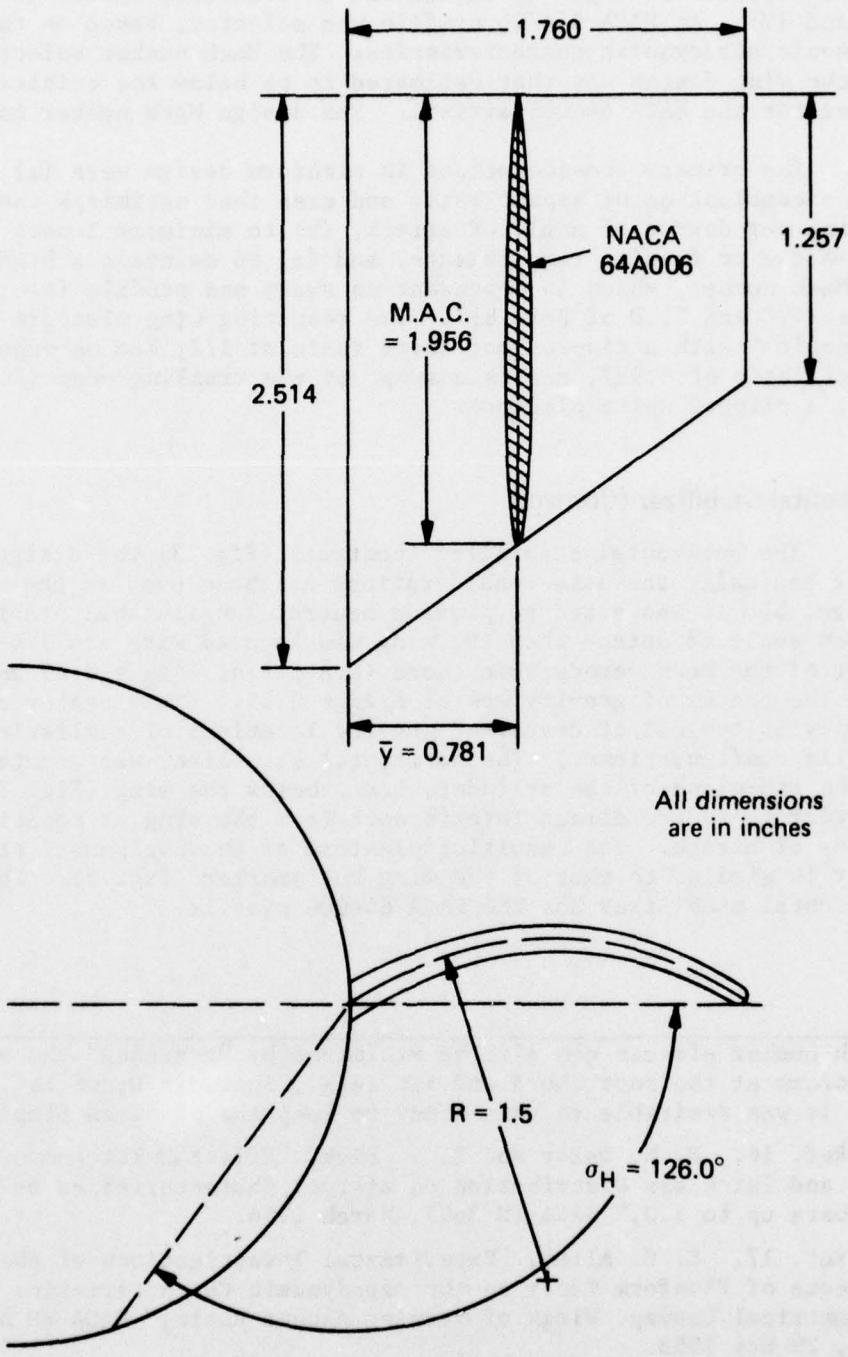

Fig. 3 Wraparound Horizontal Tail Design

Vertical Stabilizer (Control)

The vertical stabilizer (control) was sized to provide neutral directional stability when only one panel is used. The profile, projected planform, and size are the same as those of one horizontal panel.

A windward location was selected for the vertical tail (Fig. 1) for most of the testing since this location was deemed to improve the tail efficiency during pitching maneuvers; however, some tests were also conducted with the vertical tail mounted on the leeward side (Ref. 13). Most of the tests were conducted with the single planar tail mounted as shown in Fig. 1 to facilitate the analysis of the wind-tunnel data by minimizing the nonsymmetry in the x-z plane. A limited amount of testing was also conducted with a single vertical wraparound tail (Ref. 13).

BODY-WING-TAIL CONFIGURATIONS

The test configurations consisting of the components described in the previous section are shown schematically in Fig. 1. Also shown in Fig. 1 are the planar-surface configurations that were tested for comparison with the performance of the wraparound-surface configurations. The planar surfaces had the same planform as the projected planform of the wraparound surfaces. Combinations of wing longitudinal position, tail concavity orientation, tail dihedral and anhedral, and mixed configurations (wraparound wing with planar tails) were also tested. A description of the configurations tested in the longitudinal stability phase of the investigations is given in Ref. 13. Most of these configurations had the wing positioned with its 1/4-chord point of the M.A.C. at 60% of the body length (Fig. 1a), but some configurations were tested with the wing positioned with its 1/4-chord point of the M.A.C. at 50% of the body length and others at 70% of the body length. Based on the results of these tests (Ref. 19), a wraparound-surface configuration and a similar planar-surface configuration were selected for the lateral stability and the pitch-, yaw-, and roll-control test. These configurations have the wing positioned with its 1/4-chord point of the M.A.C. at $X/\ell_B = 0.50$ (Fig. 1b). Photographs of the wind-tunnel models used in the lateral stability and in the controls tests are shown in Figs. 4 and 5.

Ref. 19. E. F. Lucero, "Experimental Results of High Subsonic Aerodynamic Longitudinal Stability Characteristics of Bank-to-Turn Configurations Incorporating Wrap-Around Surfaces with Subsonic Sections," APL/JHU BFD-1-74-009, 12 February 1975.

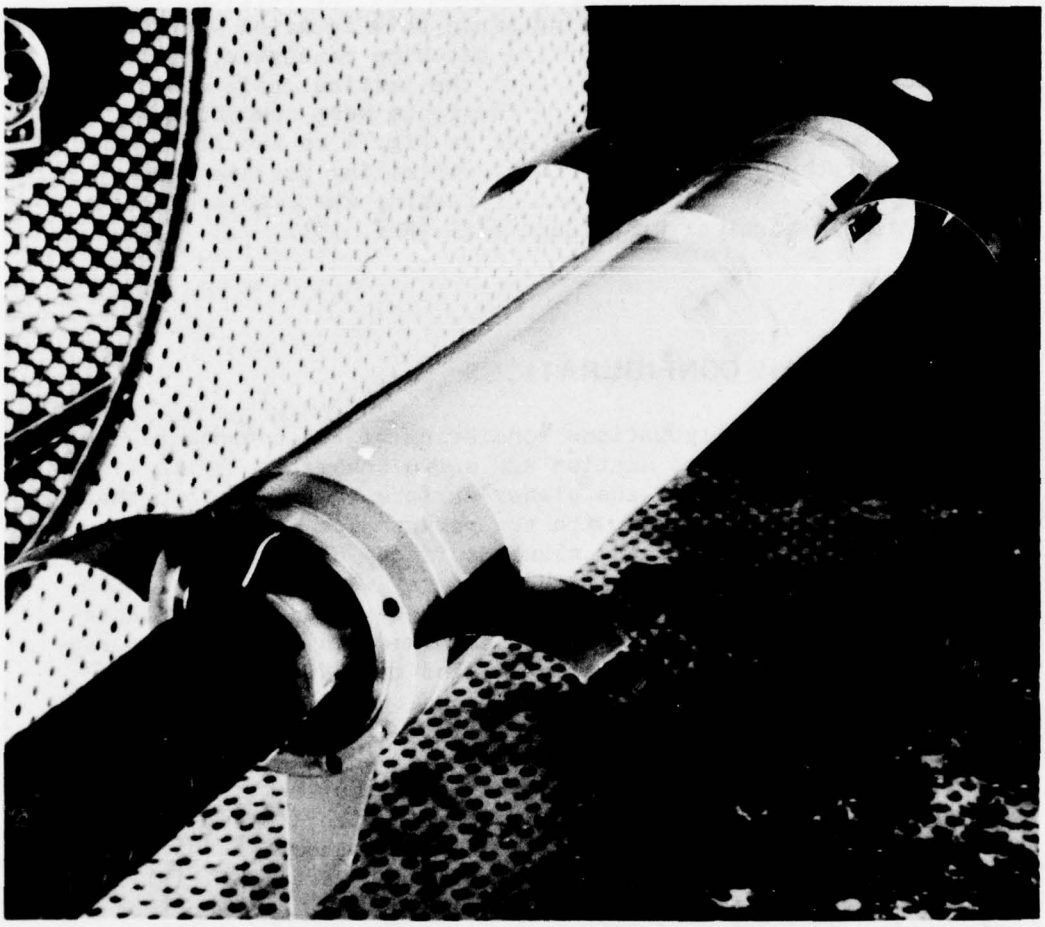

Fig. 4 Photograph of Wraparound-Surface Model

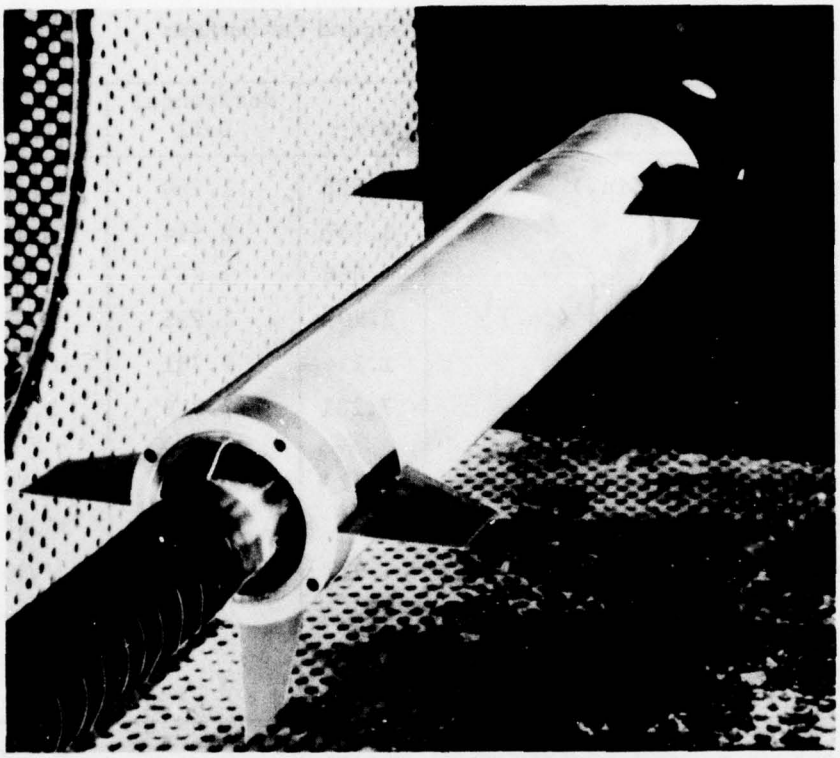

Fig. 5 Photograph of Planar-Surface Model

A summary of the pertinent dimensions and other geometric parameters of the various components of the test configurations is given in Table 1.

Table 1

Geometric Parameters of Wing and Tail Surfaces

Parameter*	Wing	Horizontal Tail	Vertical Tail
Exposed semi-span (in.)	2.598	1.760	1.760
Root chord (in.)	3.737	2.514	2.514
Tip chord (in.)	1.868	1.257	1.257
Mean aerodynamic chord (in.)	2.907	1.956	1.956
Lateral centroid (in.)	1.154	0.781	0.781
Projected surface area (one surface) (in^2)	7.281	3.318	3.318
Taper in chord	1/2	1/2	1/2
Sweep (reference)	35.6°	35.6°	35.6°
Aspect ratio (one exposed panel)	0.927	0.933	0.933
Elevation angle	30°	0°	-90°
Section profile: NACA 64A006, all surfaces			

*For the wraparound surface these geometric parameters refer to the projection of the wraparound surface on the horizontal plane containing both the root and tip chords.

3. RESULTS OF WIND-TUNNEL TESTS

The experimental program consisted of aerodynamic force and moment tests conducted in the wind tunnel, mostly at Mach 0.80. A limited amount of data was also obtained at Mach numbers ranging from 0.65 to 0.98. The freestream Reynolds number was 7.5×10^6 per foot. Results showing the main conclusions derived from this study are presented herein in terms of the aerodynamic coefficients C_N, C_m, C_Y, C_n, C_ℓ, and C_{D_o} (see Figs. 6 and 7 for direction of forces, angles, and deflections). A detailed documentation of the test results and analyses is given in Refs. 19, 20, and 21.

The presentation of the results include, where possible, (a) a comparison of the data from wraparound-surface configurations with the data from planar-surface configurations, (b) a comparison of the results with theoretical or empirical predictions, and (c) formulation of empirical approaches that could improve predictions of the aerodynamics of wraparound-surface configurations.

The results and comparisons shown for longitudinal stability characteristics are for configurations with the wing positioned with its 1/4-chord point of the M.A.C. at 60% of the body length (Fig. 1a) since most of the longitudinal stability data were obtained with the wing in this position. Based on these results of the longitudinal stability tests, the configuration with the wing positioned with its 1/4-chord point of the M.A.C. at 50% of the body length appeared to be most promising for controlling pitch. Thus, the results and comparisons shown for the lateral stability characteristics and for the control characteristics are for this 50% wind location (Figs. 1b, 4, and 5).

Ref. 20. E. F. Lucero, "Experimental Study at M = 0.8 of the Aerodynamic Controllability of the Missile Configuration for the Wrap-Around Surface Project (WASP)," APL/JHU BFD-1-75-006, 8 May 1975.

Ref. 21. E. F. Lucero, "Wrap-Around Surface Project (WASP) Studies — Analysis of Experimental Data on Lateral Stability and on Effects of Sideslip on Yaw and Roll Control, M = 0.8," APL/JHU BFD-1-75-010, 30 May 1975.

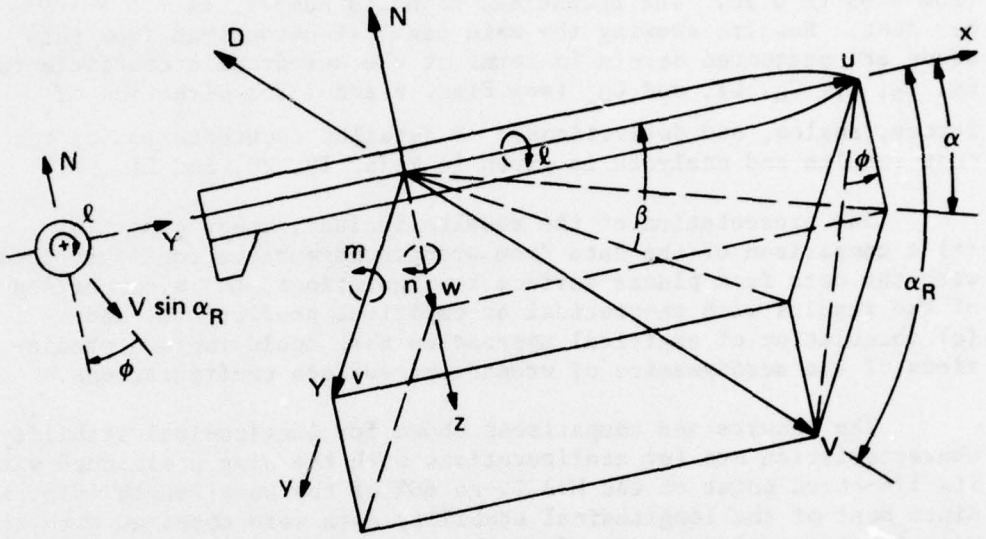

$$\vec{V} = \vec{u} + \vec{v} + \vec{w}$$

$$\tan \phi = \tan \beta / \tan \alpha$$

$$\tan^2 \alpha_R = \tan^2 \alpha + \tan^2 \beta$$

Fig. 6 Definition of Forces, Moments, and Angles

Pitch

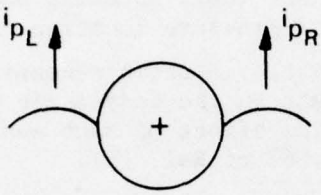

$$i_p = \frac{i_{p_L} + i_{p_R}}{2}$$

Yaw

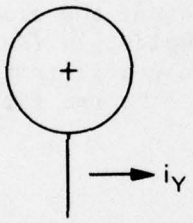

Roll

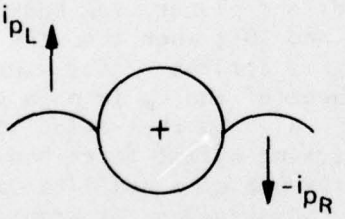

$$\delta = \frac{i_{p_L} - i_{p_R}}{2}$$

Views looking upstream
(positive deflection has leading edge in direction of arrow)

Fig. 7 Definition of Control Surface Deflections

LONGITUDINAL STABILITY

Body Alone

The normal force coefficient (C_N), pitching moment coefficient ($C_{m_{0.55}}$), and the center-of-pressure location ($X_{c.p.}$) for the von Karman nose-cylinder body, which is shown schematically in Fig. 1, are given in Fig. 8. Data on the body alone were also obtained at Mach 0.90 and 0.95. The effect of Mach number is small in this Mach-number range (see Fig. 63 of Ref. 19).

Empirical predictions of the aerodynamic characteristics of the body can be made from data available in the literature on similar bodies. The empirical predictions shown in Fig. 8 are based on test data (Ref. 22) on a body having a tangent ogive nose of fineness ratio 1.75 and an overall fineness ratio 10.94. The agreement with the data of the present body, which has a fineness ratio 10.0 and a von Karman nose of fineness ratio 2.1, is excellent. Where data on similar bodies cannot be found, the cross-flow theory of Allen and Perkins, as modified by Goldstein (Ref. 23), provides a good prediction of the normal force coefficient, but the center-of-pressure location is predicted to be too far forward on the body (Fig. 8).

Body-Wing

No significant difference was observed between the C_N (or C_m) data of the wraparound wing-body and planar wing-body configurations when the wing is high (Figs. 9 and 10); when the wing is low (convex surface windward) C_N is higher for the planar wing when the angle of attack, α, is above about 8° and C_m is more positive for the curved wing beginning at $\alpha \approx 4°$. In the region of agreement, any method for accurately predicting normal force and pitching moment of planar wings (in the presence of a body) can also be used to obtain reasonable estimates of these values for wraparound wings provided that the projected planforms are the same for the planar and wraparound wings. For example, the method of Polhamus (Ref. 24) in

---

Ref. 22. E. C. Polhamus, "Effect of Nose Shape on Subsonic Aerodynamic Characteristics of a Body of Revolution Having a Fineness Ratio of 10.94," NACA RM L57 F25, 12 August 1957.

Ref. 23. Handbook of Supersonic Aerodynamics, Bodies of Revolution, NAVWEPS Report 1488 (Vol. 3, Sect. 8), October 1961.

Ref. 24. E. C. Polhamus, "Predictions of Vortex-Lift Characteristics by a Leading Edge Suction Analogy," J. Aircr., Vol. 8, No. 4, April 1971.

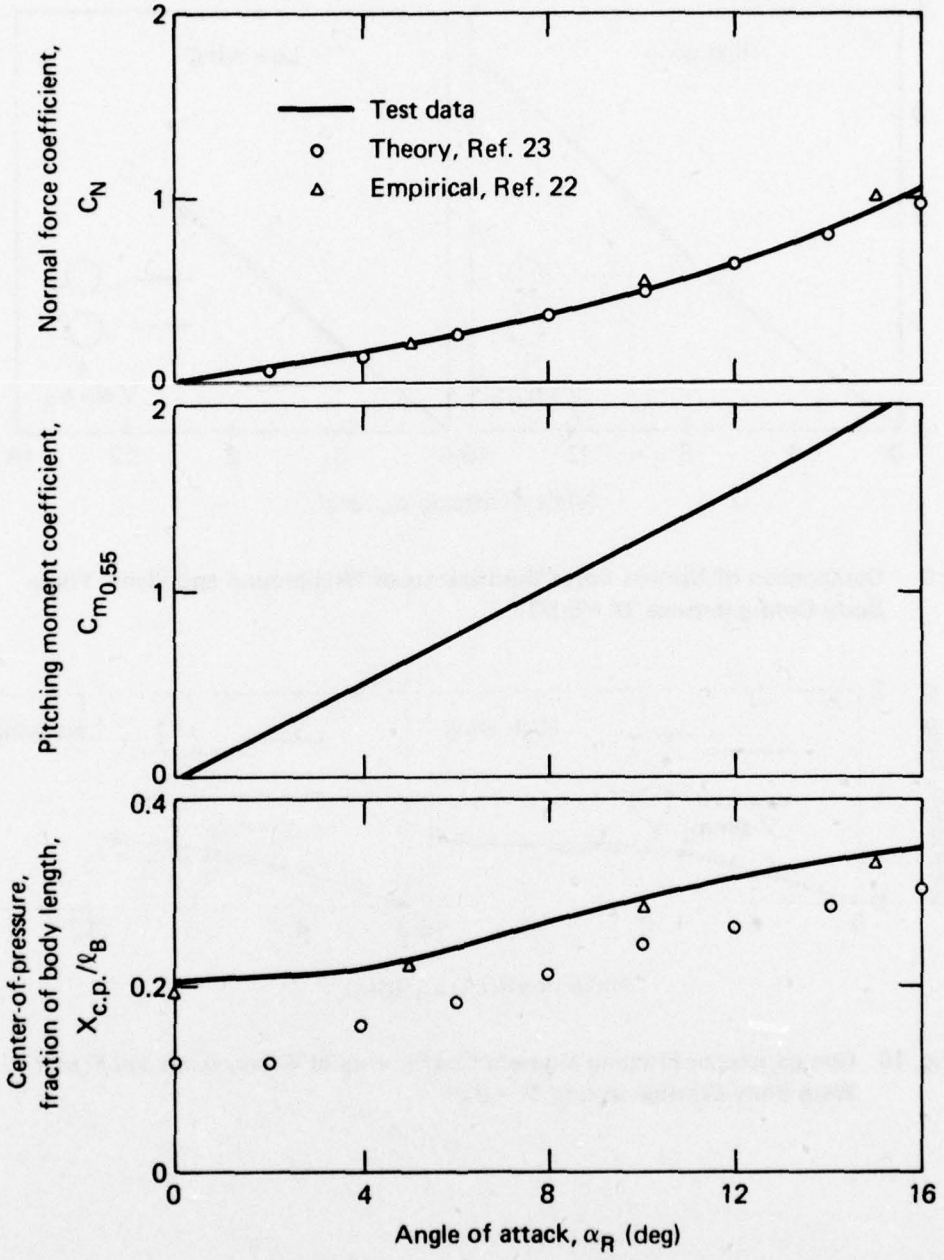

Fig. 8 Body-Alone Longitudinal Characteristics, M = 0.80

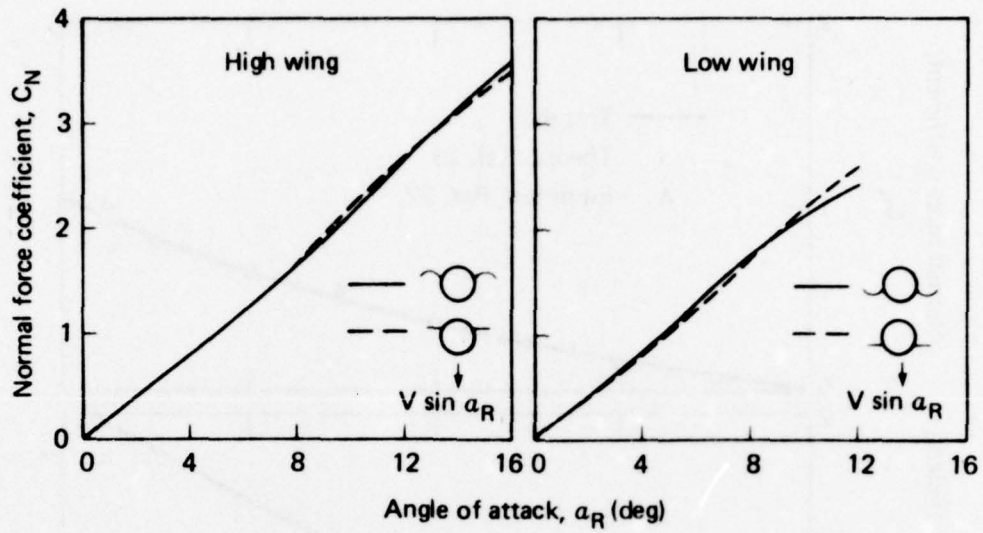

Fig. 9 Comparison of Normal Force Coefficients of Wraparound and Planar Wing-Body Configurations, M = 0.80

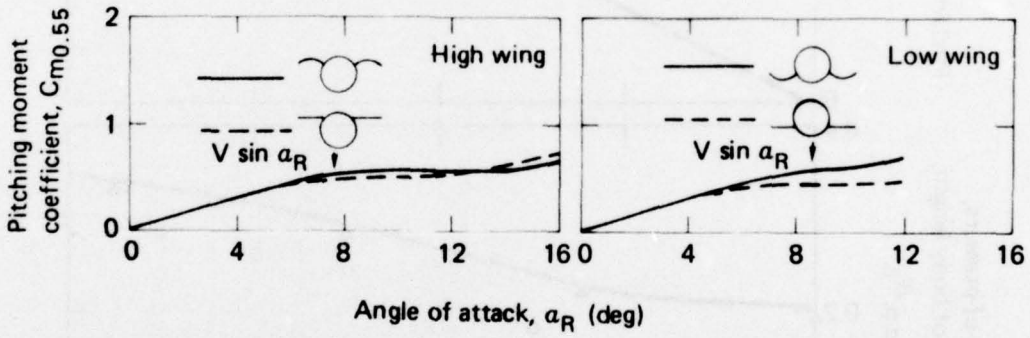

Fig. 10 Comparison of Pitching Moment Coefficients of Wraparound and Planar Wing-Body Configurations, M = 0.80

conjunction with slender body interference factors (Ref. 10) gives a good prediction of the wing-normal force coefficient plus mutual body-wing interference (Fig. 11). The coefficient $C_{N_{W+W_B+B_W}}$ includes the normal force on the wing plus the wing-body interference effects on body and wings. From test data, $C_{N_{W+W_B+B_W}} \equiv C_{N_{BW}} - C_{N_B}$. Lifting surface theory (Ref. 9) was found to predict accurately the slope of C_N versus α at $\alpha = 0$. For center-of-pressure estimates, test data indicate that the 1/4-chord point of the M.A.C. would be a reasonable engineering estimate in the Mach number and angle of attack range tested.

In the longitudinal investigations described above, the wing was positioned with its 1/4-chord point of the M.A.C. at 60% of the body length. Body-wing configurations with the wing positioned with its 1/4-chord point at $X/\ell_B = 0.50$ and $X/\ell_B = 0.70$ were also investigated and no significant differences in C_N due to wing position were observed (see Fig. 53 of Ref. 19).

Body-Tail

A similar comparison of the body-tail data (Figs. 12 and 13) also shows little difference between the longitudinal stability characteristics of the wraparound and the planar tails, that have the same planform, although wraparound tails provide slightly more stability at high positive angle of attack.

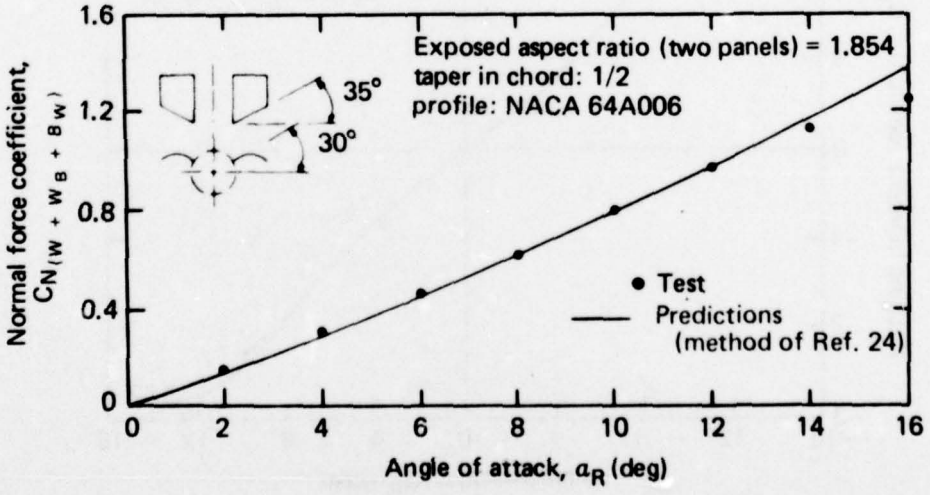

Fig. 11 Comparison of Experimental and Predicted Normal Force Coefficients of Wraparound Wings (including interference), M = 0.80

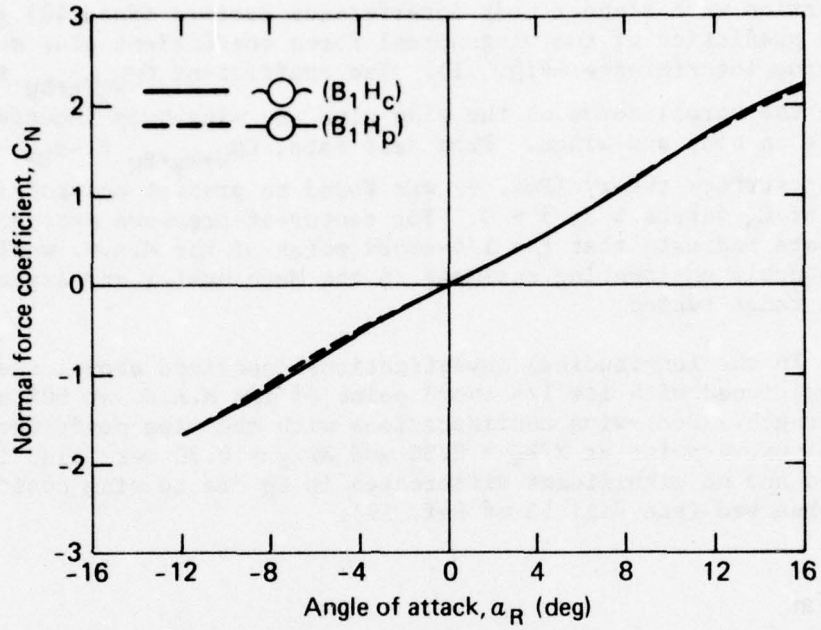

Fig. 12 Comparison of Normal Force Coefficients of Wraparound and Planar Tail-Body Configurations, M = 0.80

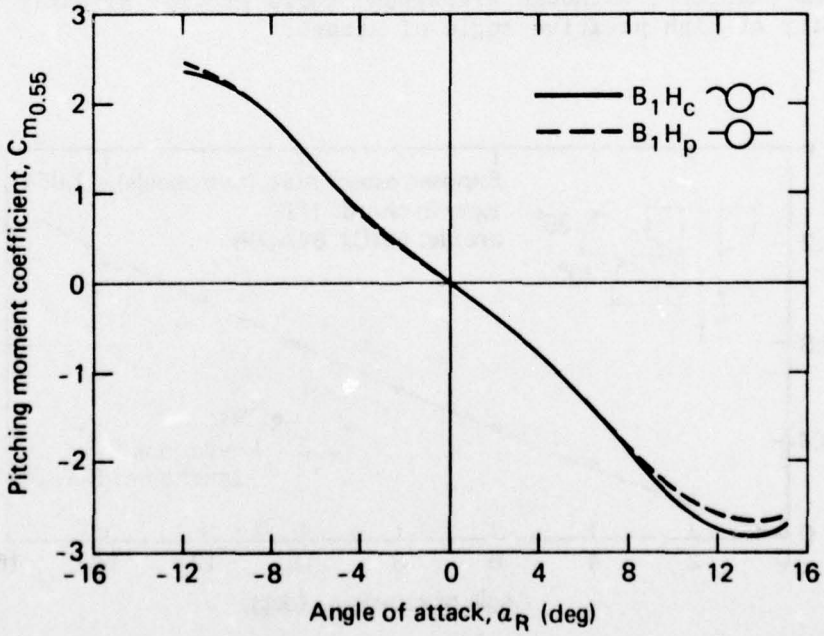

Fig. 13 Comparison of Pitching Moment Coefficients of Wraparound and Planar Tail-Body Configurations, M = 0.80

Full-Configuration Data

The full configuration using wraparound surfaces has essentially the same values of C_N as the full configuration using planar surfaces up to $\alpha \approx 12°$ when the wing is high and up to $\alpha \approx 8°$ when the wing is low (Fig. 14); the stability of the wraparound configuration is equal to or higher (C_m more negative) than the stability of the planar-surface configuration (Fig. 15) when the wing is high. The low-wing (concave side leeward), wraparound configuration is much less satisfactory than the high-wing (concave side windward) wraparound configuration in that at a given α it has a lower value of C_N (Fig. 16) and less longitudinal stability. Thus, in the most likely operating range of angle of attack (positive α) the wraparound-surface configuration with the high wing is more aerodynamically desirable than either the wraparound-surface configuration

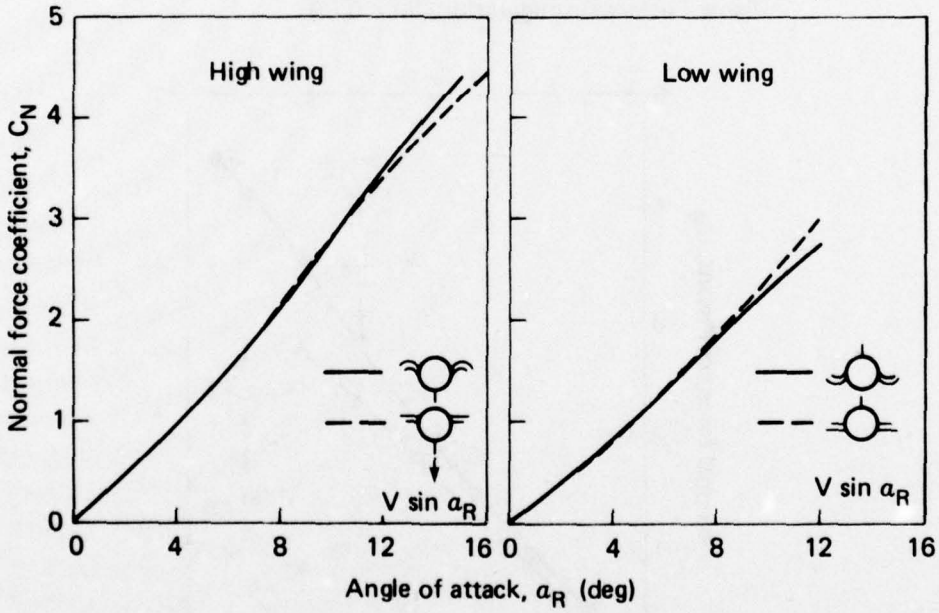

Fig. 14 Comparison of Normal Force Coefficients of Full Wraparound- and Planar-Surface Configurations, M = 0.80

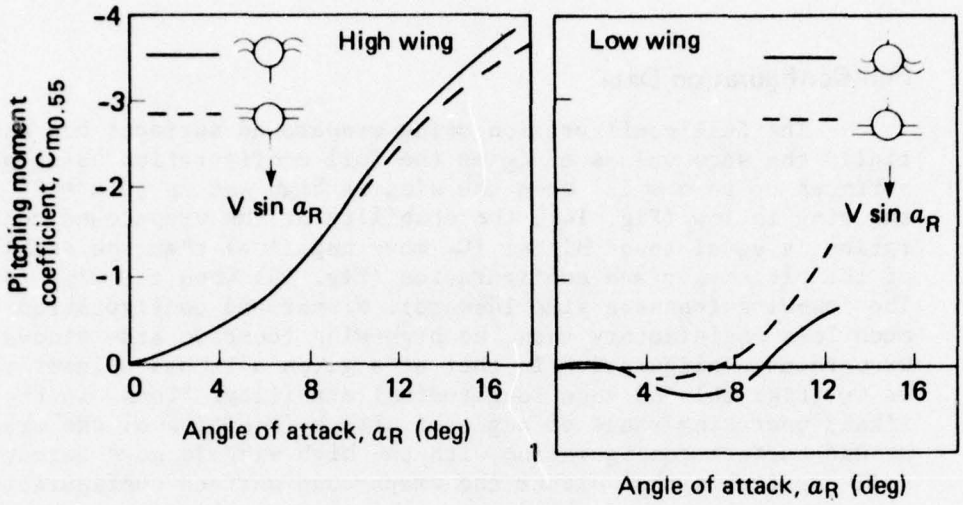

Fig. 15 Comparison of Pitching Moment Coefficients of Full Wraparound- and Planar-Surface Configurations, M = 0.80

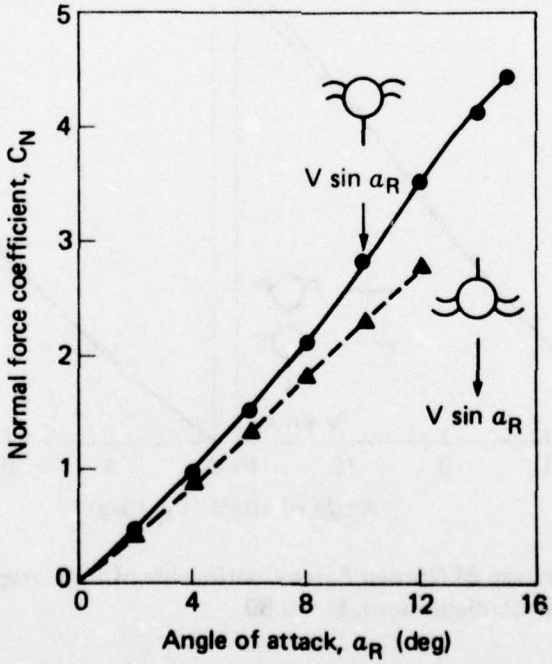

Fig. 16 Effect of Concavity Orientation and Wing Elevation on Normal Force Coefficient of the Full Configuration, M = 0.80

with the low wing or the configuration that has all planar surfaces. Several other wraparound-surface configurations tested were not as desirable aerodynamically as the high-wing configuration (Ref. 19). Further discussion in this report will be confined, therefore, to the high-wing configuration.

The contributions of the various components of the full configurations (both wraparound and planar) to C_N and C_m are summarized in Figs. 17 and 18. The presence of the vertical tail did not change the C_N or C_m of the various components.

The longitudinal centers-of-pressure of the body-wing-tail configurations are given in Fig. 19; the centers-of-pressure of the various configurational components are given in Fig. 20.

Efficiency of Tails for Longitudinal Stabilization

When the horizontal tail stabilizer is within the wing wake, its stabilizing effectiveness is reduced because of the wing downwash. The ratio of the pitching moment contribution from the tail with the wing present to that obtained when the wing is not present is the tail efficiency, η_{HV}. A comparison of this parameter for the wraparound- and planar-surface configurations shows (Fig. 21) that the tails of the wraparound-surface configuration are more efficient stabilizers than the tails of the planar-surface configuration. The experimental data from the wraparound-surface configuration are compared in Fig. 22 with (a) the values of η_{HV} calculated using Decker's downwash formulation derived for planar surfaces (Ref. 11), i.e.,

$$\eta_{HV} = (q_\ell/q)\ (1 - \frac{d\bar{\varepsilon}}{d\alpha}) ,$$

and (b) with the same formulation of $d\bar{\varepsilon}/d\alpha$ but modified by an "effective tail height" parameter, $h_{t(eff)}$, based on the geometry of the wraparound surfaces (Fig. 22). An improvement in the predicted value of η_{HV} for the wraparound-surface configuration is obtained when $h_{t(eff)}$ is used. The details of the empirical derivation of $h_{t(eff)}$ and of its use as a correlation parameter for the interference between the wing vortices and the tail are discussed in Ref. 19.

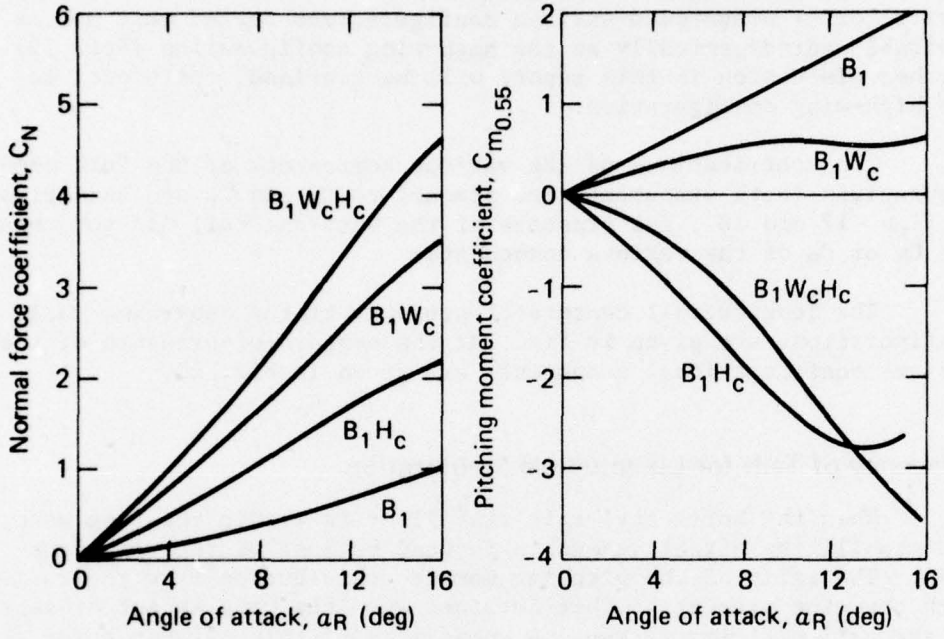

Fig. 17 Summary of Component C_N and C_m, Wraparound-Surface Configurations, M = 0.80

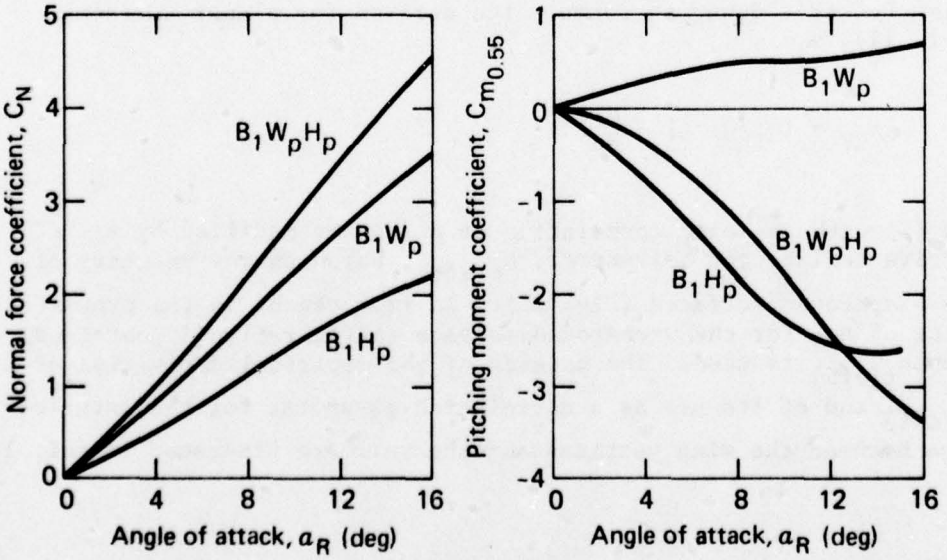

Fig. 18 Summary of Component C_N and C_m, Planar-Surface Configurations, M = 0.80

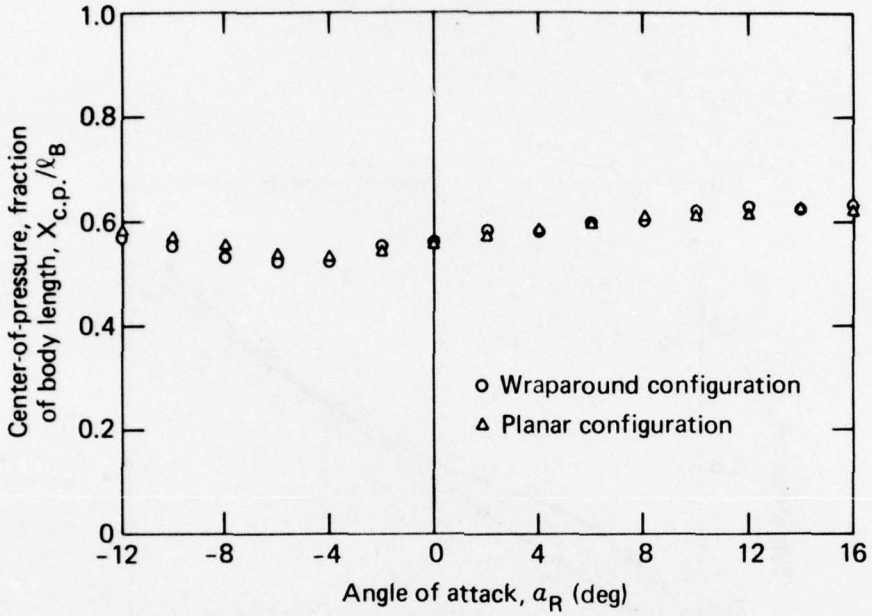

Fig. 19 Comparison of Centers-of-Pressure of Full Wraparound- and Planar-Surface Configurations, M = 0.80

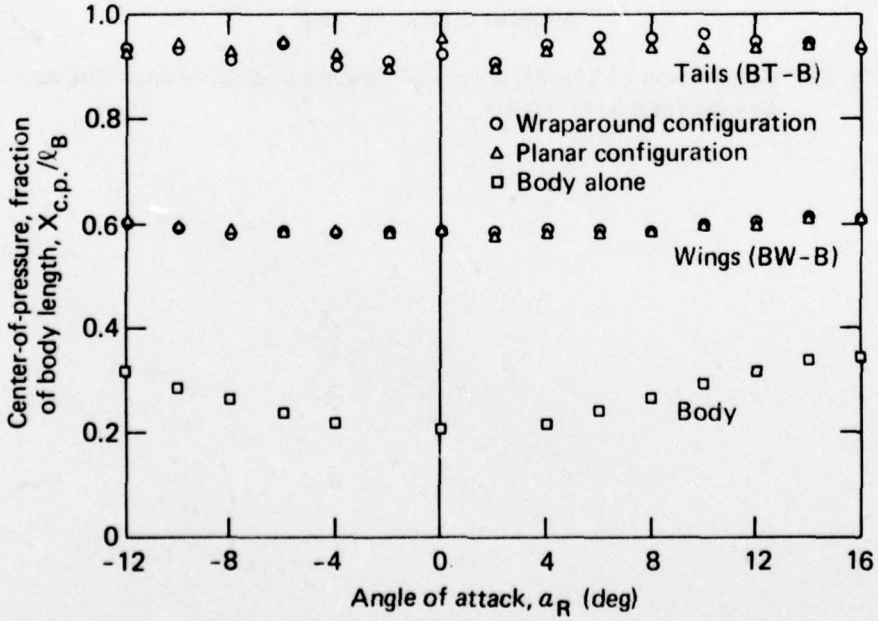

Fig. 20 Summary of Component Center-of-Pressure, M = 0.80

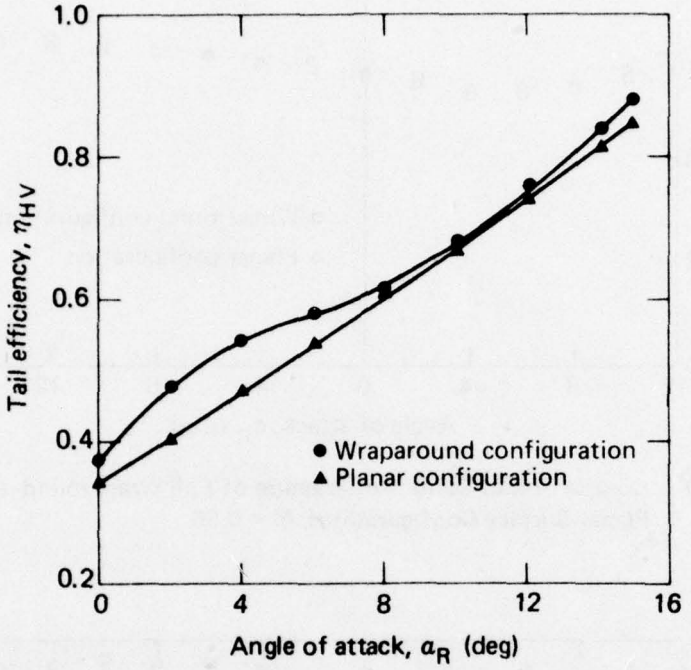

Fig. 21 Comparison of Tail Efficiency of Wraparound- and Planar-Surface Configurations, M = 0.80

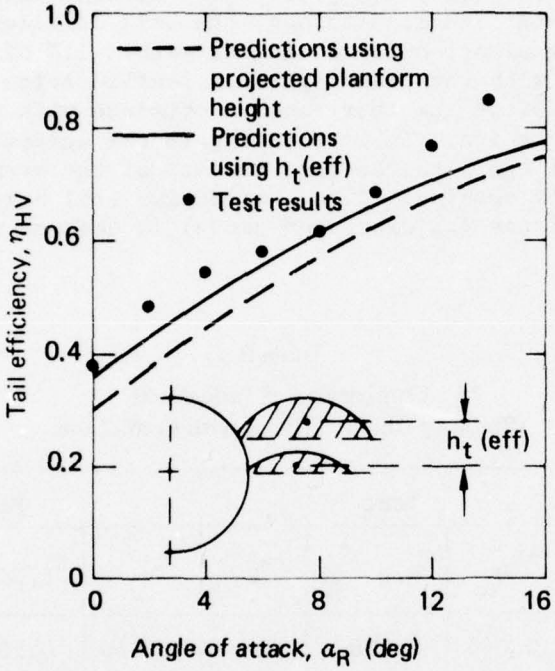

Fig. 22 Comparison of Experimental and Predicted Tail Efficiency of Wraparound-Surface Configuration, M = 0.80

Comparison of Linearized Characteristics with Predictions

A comparison of the predicted values of C_{N_α} and $X_{c.p.}$ at $\alpha = 0°$ with the test results obtained at Mach 0.8 for the various components shows that prediction procedures using planar-surface methods are satisfactory for preliminary design (Table 2). For the full body-wing-tail configurations, the tail efficiency, η_{HV}, is predicted using planar-surface methods within 11% of the test results obtained with the planar-surface configuration and within approximately 26% of the test results obtained with the wraparound-surface configuration. An improvement in the agreement of the predicted value of η_{HV} with the test results of the wraparound-surface configuration is obtained if the "effective tail height" deduced for wraparound surfaces (as discussed above) is used to calculate η_{HV}

Table 2

Comparison of Linearized Stability Characteristics with Predictions

Component	Test			Predicted			
	*C_{N_α}	$X_{c.p.}/\ell_B$	η_{HV}	C_{N_α}	$X_{c.p.}/\ell_B$	η_{HV}	Ref.
B_1	0.040	0.208	-	0.040	0.207	-	22
$B_1W_P - B_1$	0.154	0.585	-	0.152	0.594	-	9, 10
$B_1W_C - B_1$	0.166	0.584	-	0.152	0.594	-	
$B_1H_P - B_1$	0.080	0.937	-	0.081	0.940	-	9, 10
$B_1H_C - B_1$	0.086	0.921	-	0.081	0.940	-	
*$B_1V_1 - B_1$	-0.040		-	-0.041		-	9, 10
Planar surface BWHV configuration			0.329			0.295	11
Wraparound surface, BWHV configuration			0.395			0.360†	11, 19

*For BV - B, C_{Y_β} is given instead of C_{N_α}.

†Using "effective tail height" for wraparound surfaces.

instead of using the planar-surface height. With this method, the value of η_{HV} is predicted within 9% of the test results.

LONGITUDINAL CONTROL

Longitudinal control is obtained by deflection of the horizontal tails as depicted in Fig. 7. Tests were conducted with positive and negative control surface deflections. The test values of the pitch-control surface deflection, i_p, are shown in Fig. 22. When the wraparound tails are deflected to negative values of i_p (i.e., convex side windward at $\alpha = 0$) the magnitudes of the control force and moment per degree of control surface deflection, $\Delta C_N/i_p$ and $\Delta C_m/i_p$, respectively, are generally greater than those of the planar tails (Fig. 23). When the wraparound tails are deflected to positive values of i_p, i.e., concave side windward, the magnitudes of $\Delta C_N/i_p$ and $\Delta C_m/i_p$ are generally less than those of the planar tails. When the convex side of the wraparound tails is windward a larger control moment is obtained than when the concave side is windward. This situation is desirable since (for steady-state conditions) a stable missile in cruise flight would normally be flying with a negative value of control-surface deflection. Thus for the expected operating range of angle-of-attack and control-surface deflection for a stable missile, the wraparound tails have a pitch control effectiveness that is generally greater than that of the planar tails.

The data on control effectiveness for both wraparound- and planar-surface configurations correlates as almost a single-valued function of the local tail angle-of-attack, α_H (Fig. 24), for both body-tail and body-wing-tail configurations. It is therefore suggested that, for a given body-wing-tail configuration having wraparound surfaces, the control effectiveness parameter, $\Delta C_m/i_p$, can be obtained empirically from a plot of $\Delta C_m/i_p$ versus α_H obtained from the data from a body-tail configuration. The applicable value of α_H for the body-wing-tail configuration is obtained from $\alpha_H = \alpha_R + i_p - \bar{\varepsilon}$. The average downwash angle $\bar{\varepsilon}$ is calculated using the proper value of $h_{t(eff)}$ for the given wraparound-surface configuration (Ref. 19). In the absence of body-tail data, predictive methods derived for planar surfaces provide a reasonable estimate of $\Delta C_m/i_p$ for preliminary design (see curve in Fig. 24). The predicted values shown in Fig. 24 were calculated using the leading edge suction analogy (Ref. 24) with account made for body-tail interference by using slender body interference factors (Ref. 10). Note that ΔC_m is the difference between the value of C_m at $i_p \neq 0$

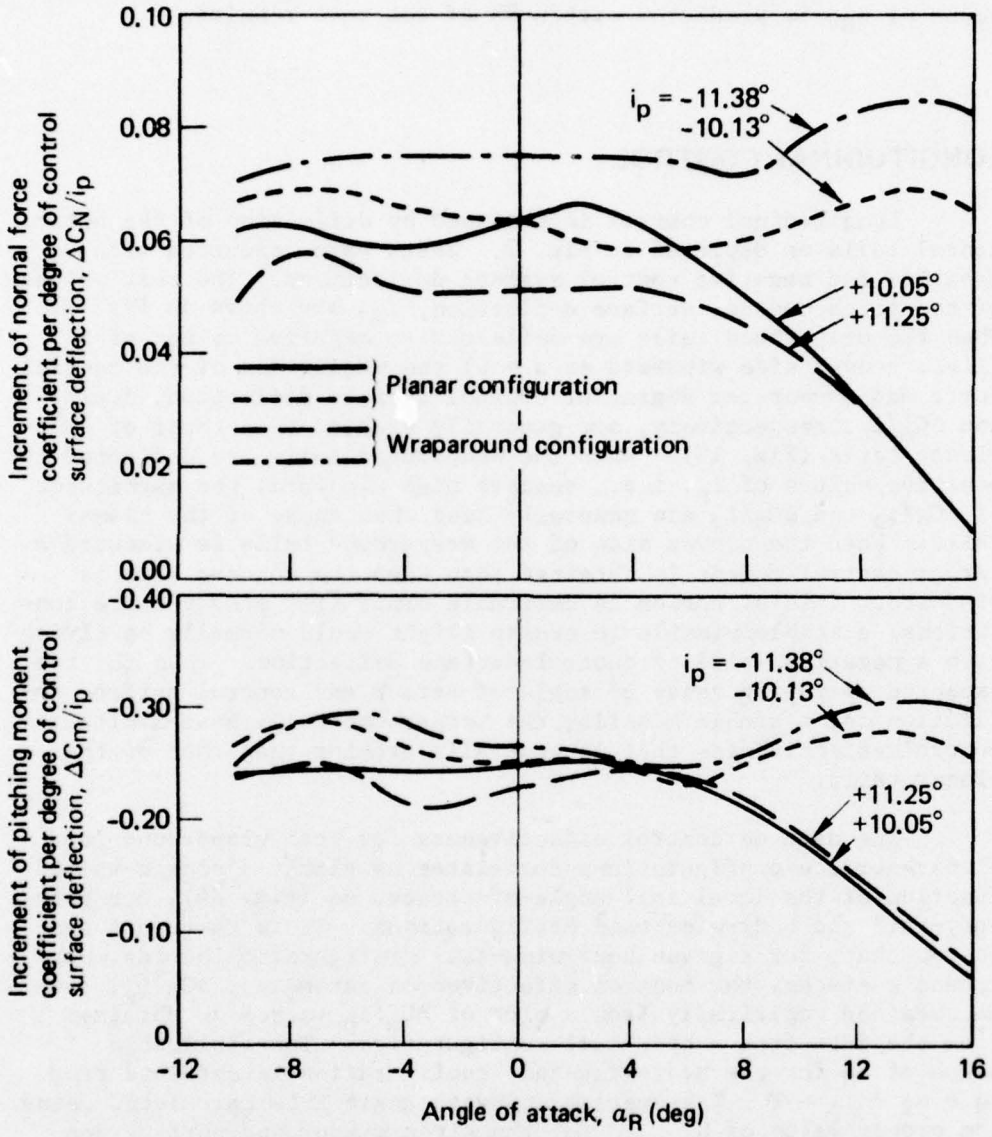

Fig. 23 Comparison of Control Characteristics of Wraparound- and Planar-Surface Configurations, M = 0.80

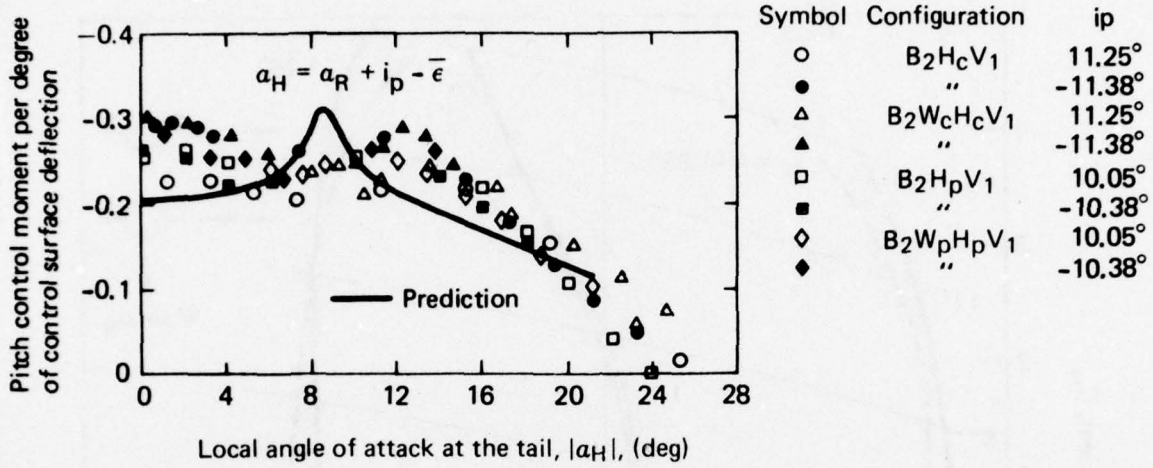

Fig. 24 Correlation of Pitch Control Effectiveness with Angle of Attack at the Tail, M = 0.80

and its value at $i_p = 0$. The predicted value of $\Delta C_m/i_p$ is generally lower than that obtained from the present data and thus provides a conservative value of $\Delta C_m/i_p$.

Note from the data correlation in Fig. 24 that pitch control effectiveness declines beginning at $\alpha_H \approx 12°$, but some control moment is available to $\alpha_H \approx 24°$.

LONGITUDINAL TRIM CHARACTERISTICS

A summary plot showing the static longitudinal stability and control characteristics of both the wraparound-surface and planar surface configurations is given in Fig. 25. These configurations have the wing positioned one diameter forward of the configurations discussed earlier in this section (i.e., the 1/4-chord point of the M.A.C. at 0.50 ℓ_B). These configurations are slightly unstable at $\alpha = 0°$, $C_N = 0$; i.e., $dC_m/dC_N > 0$ at $C_N = 0$. These configurations were chosen for the control studies because the results of the longitudinal stability studies (see Longitudinal Stability) indicated that it has promising controllability with small "trim" control

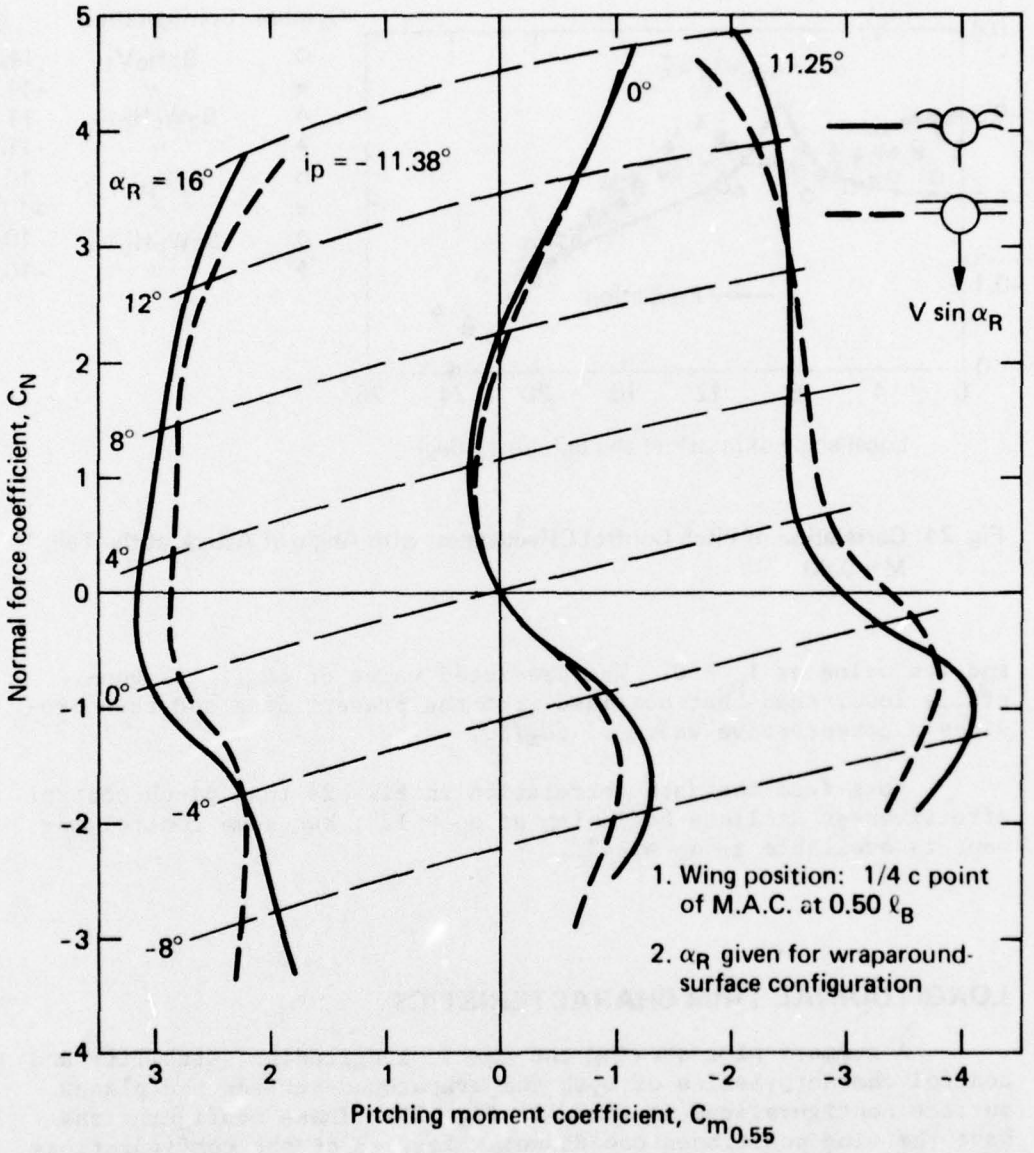

Fig. 25 Comparison of Longitudinal Stability and Control Characteristics of Wraparound- and Planar-Surface Configurations, M = 0.80

surface deflection. The missile is in trim when $C_m = 0$, i.e., the points along the ordinate are trim points for a center of gravity position at 0.55 ℓ_B from the nose.

The "trim" maneuverability and control characteristics for a center-of-gravity position at 55% of the body length are shown in Fig. 26 for both wraparound-surface and planar-surface configurations. The maneuverability factor shown in Fig. 26 is a figure of merit indicating the capability of the missile to change its flight path. It is the ratio of the maneuver achievable at a given angle-of-attack to the maneuver available for the wraparound configuration at a 16° angle-of-attack. As an example, a 4-g maneuver would be available at 16° angle-of-attack for a missile of the proportion of the wraparound-surface configuration that is 1 ft in diameter, 10 ft long, weighing 800 lb, and flying at sea level at Mach 0.8. Similarly, a 1-g maneuver would be available at $\alpha = 16°$ for the wraparound-surface configuration at an altitude of 34 000 ft. (Note that the wraparound-surface configuration has a maneuver capability that is slightly greater than that of the planar-surface configuration.) The tail control deflections needed to hold either the wraparound- or planar-surface configuration at the desired angle-of-attack are less than $|5°|$. Thus the wraparound-surface configuration is aerodynamically feasible from the standpoint of longitudinal trim characteristics.

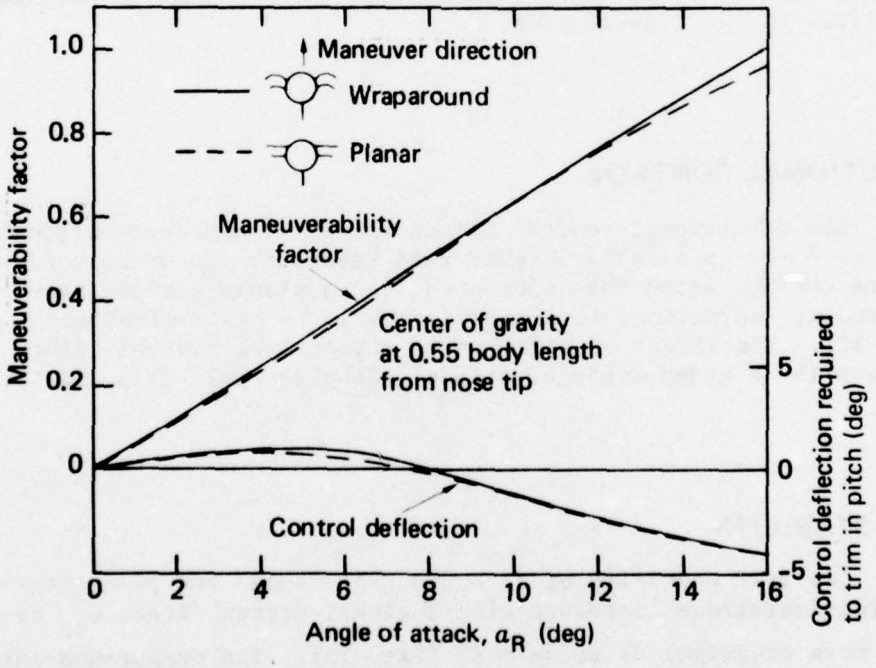

Fig. 26 Comparison of the Trim Maneuverability and Control Characteristics of Wraparound- and Planar-Surface Configurations, M = 0.80

DIRECTIONAL STABILITY

The wraparound-surface configuration has directional stability characteristics that are generally more favorable (i.e., more stable) in the expected operating regime than those of the planar-surface configurations, although both appear to be satisfactory (Fig. 27). For both configurations, the yawing moment coefficient, C_n, varies linearly or increases monotonically with sideslip angle, β (Fig. 28), except at $\alpha_R = 12.7°$ where C_n for the wraparound-surface configuration is highly nonlinear with β.

A compilation and an analysis of the contribution of the various components to directional stability of the wraparound-surface configuration are given in Ref. 21. An important result obtained from these component data is that, for a body-vertical-tail, the effectiveness of the vertical stabilizer in providing directional stability is significantly reduced when it is located in the leeward flow (Fig. 29). Thus for this configuration, the windward location for a vertical stabilizer is more desirable than the leeward location. It is not known whether the same leeward degradation in directional stability exists for the body-wing-tail configuration, since directional stability data were not obtained with the full high-wing configuration having the vertical stabilizer on the leeward side.

DIRECTIONAL CONTROL

The directional control effectiveness of a planar vertical panel at $\beta = 0$ is slightly higher when used with the wraparound-surface configuration than when used with a planar-surface configuration; and neither is affected greatly by angle-of-attack (Fig. 30). The effect of sideslip on directional control effectiveness (at a given angle-of-attack), is also small (Fig. 31).

ROLL STABILITY

The roll stability of both the wraparound- and planar-surface configurations increases with angle-of-attack (i.e., C_{ℓ_β} becomes more negative) up to $\alpha_R \approx 8°$ (Fig. 32). The wraparound-surface configuration is more stable in roll than the planar-surface

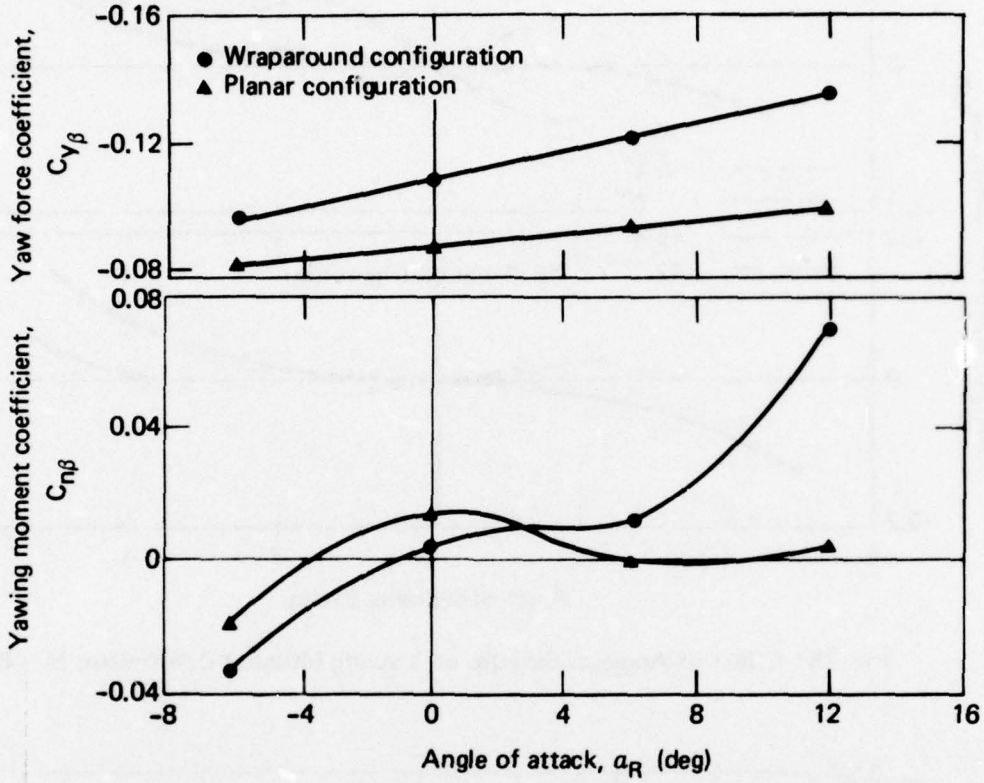

Fig. 27 Comparison of Directional Stability Derivatives of Wraparound- and Planar-Surface Configurations; M = 0.80, $\beta = 0°$, $X_{c.g.}/\ell_B = 0.55$

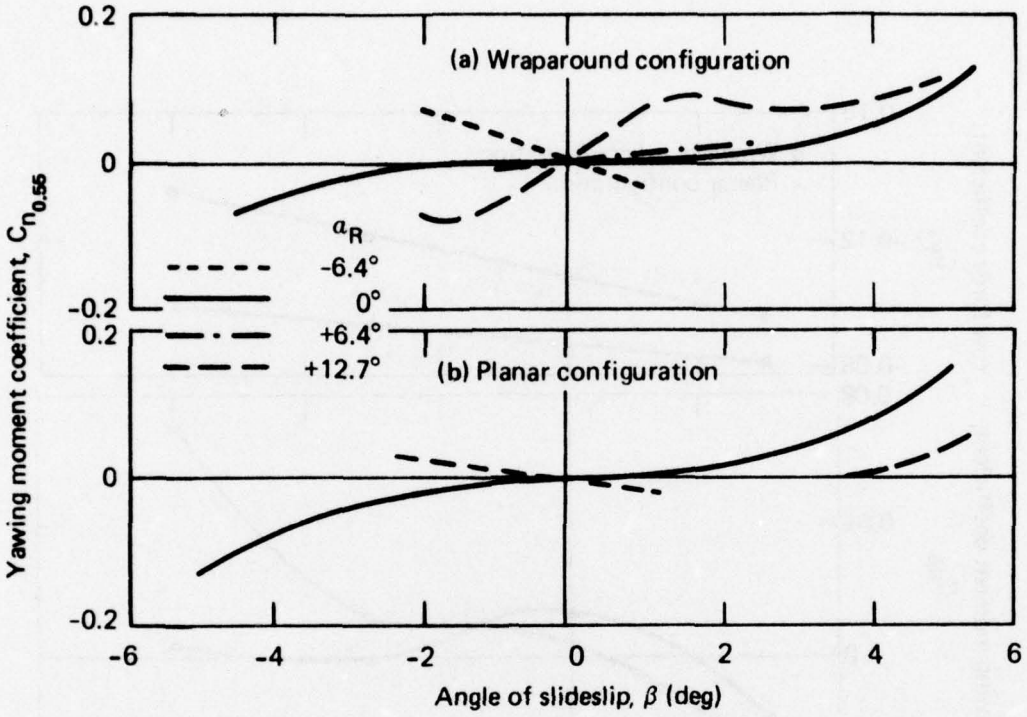

Fig. 28 Effect of Angle of Sideslip on Yawing Moment Coefficient, M = 0.80

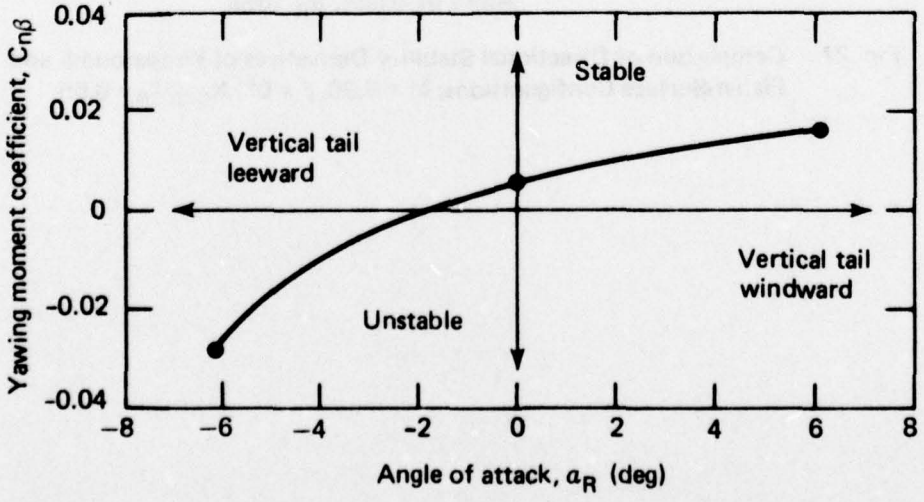

Fig. 29 Effect of Location of Vertical Tail on Directional Stability (Body-Vertical Tail Configuration); M = 0.80, $X_{c.g.}/\ell_B = 0.55$

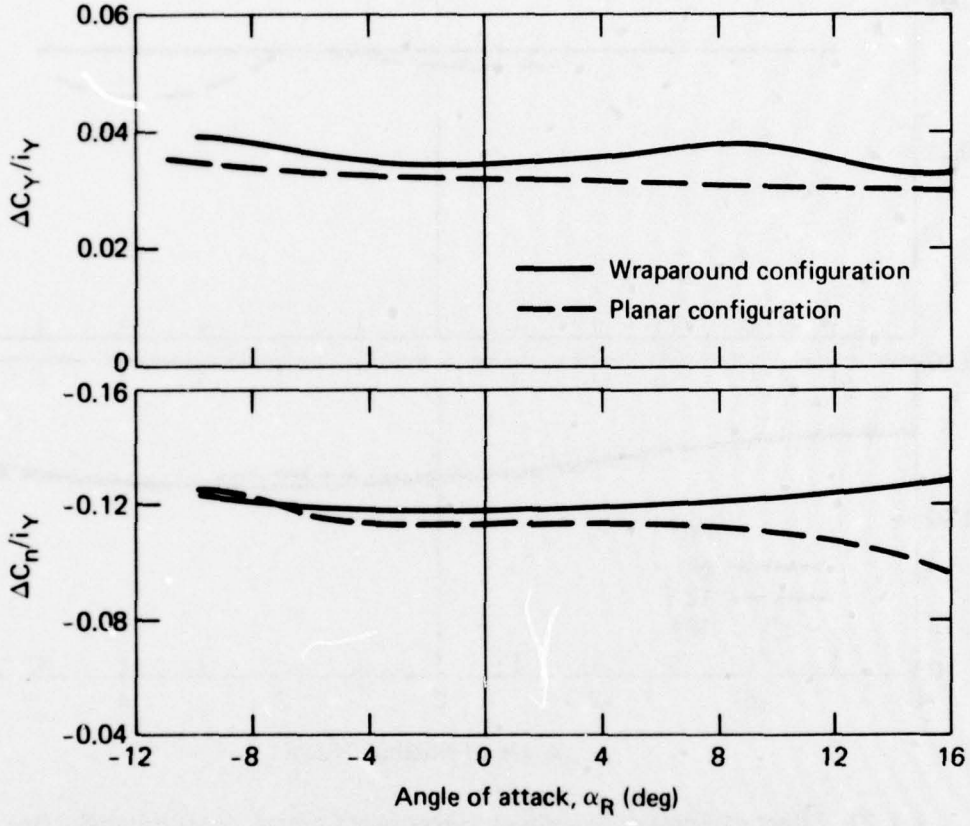

Fig. 30 Comparison of Directional Control Effectiveness of Wraparound- and Planar-Surface Configurations; M = 0.80, $X_{c.g.}/\ell_B = 0.55$, $\beta = 0°$

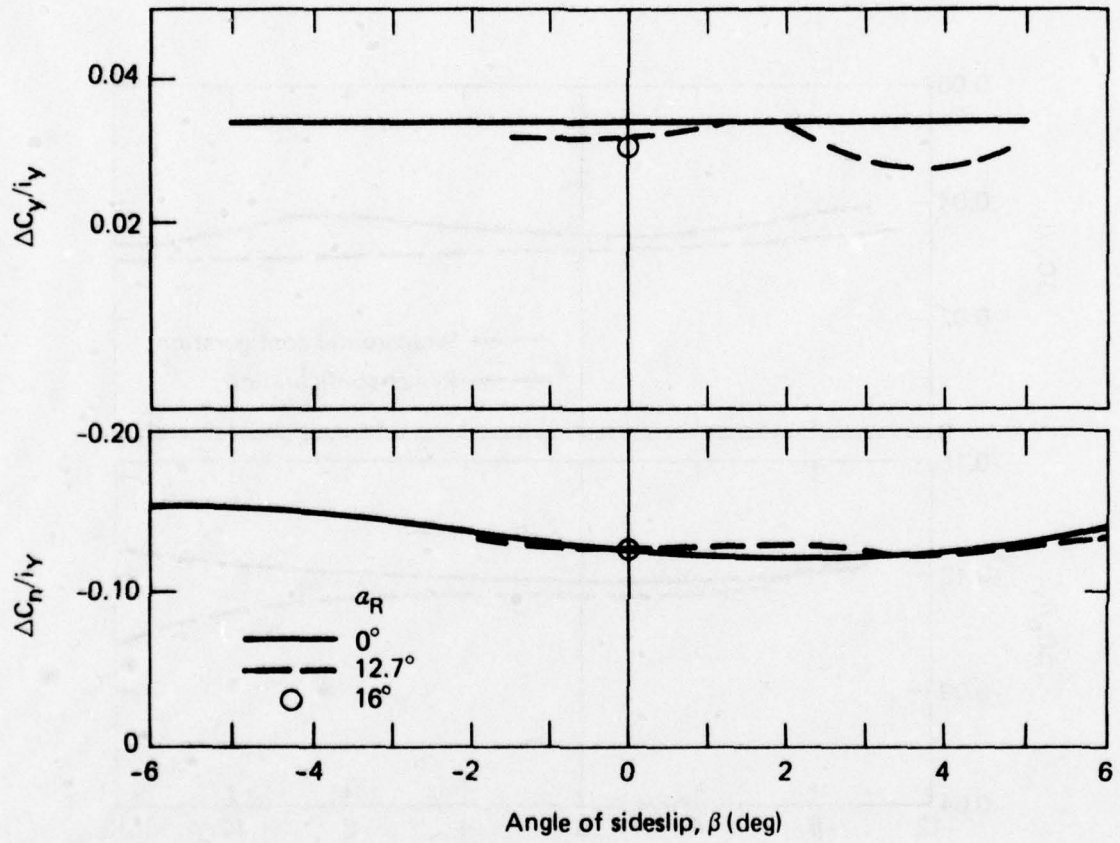

Fig. 31 Effect of Angle of Sideslip on Directional Control, Wraparound-Surface Configuration; M = 0.80, $X_{c.g.}/\ell_B = 0.55$

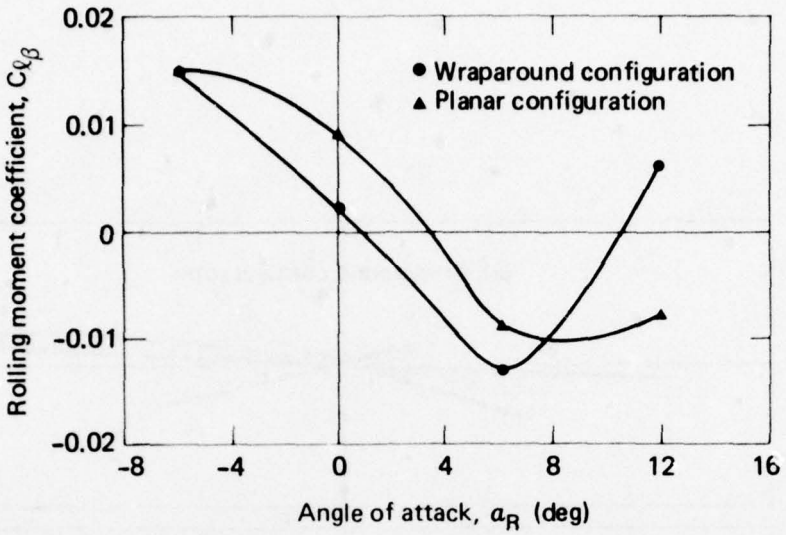

Fig. 32 Comparison of Roll Stability Derivatives of Wraparound- and Planar-Surface Configurations; M = 0.80, $\beta = 0°$

configuration for angles-of-attack up to 8°. The data at $\alpha = 0°$ from the body-wing configuration (see Table IV of Ref. 19) show that the wraparound wings produce 1.6 times more roll stability than the planar wings. Thus, the wraparound wings may be the source for the higher roll stability of the wraparound-surface configuration. At both $\alpha = 0°$ and $\alpha = 6°$, the stability in roll generated by the wraparound wings more than counteracts the instability in roll generated by the vertical fin.

At $\alpha_R \simeq 8°$, the wraparound-surface configuration exhibits decreasing roll stability and becomes unstable in roll at $\alpha_R \approx 11°$. The source for this decreasing roll stability could not be determined from the data available. The roll instability of the wraparound-surface configuration exhibited at $\alpha_R > 11.2°$ should not present any problems in controlling the missile. The results of simple calculations of control surface deflections required to trim in pitch, yaw, and roll for maneuvers at $\alpha_R = 12.7°$ verify this.

The rolling moment coefficient is fairly linear with sideslip angle, β, for both configurations (Fig. 33). The wraparound-surface configuration, however, has a slight nonlinear trend of C_ℓ with β at $\alpha_R = 12.7°$.

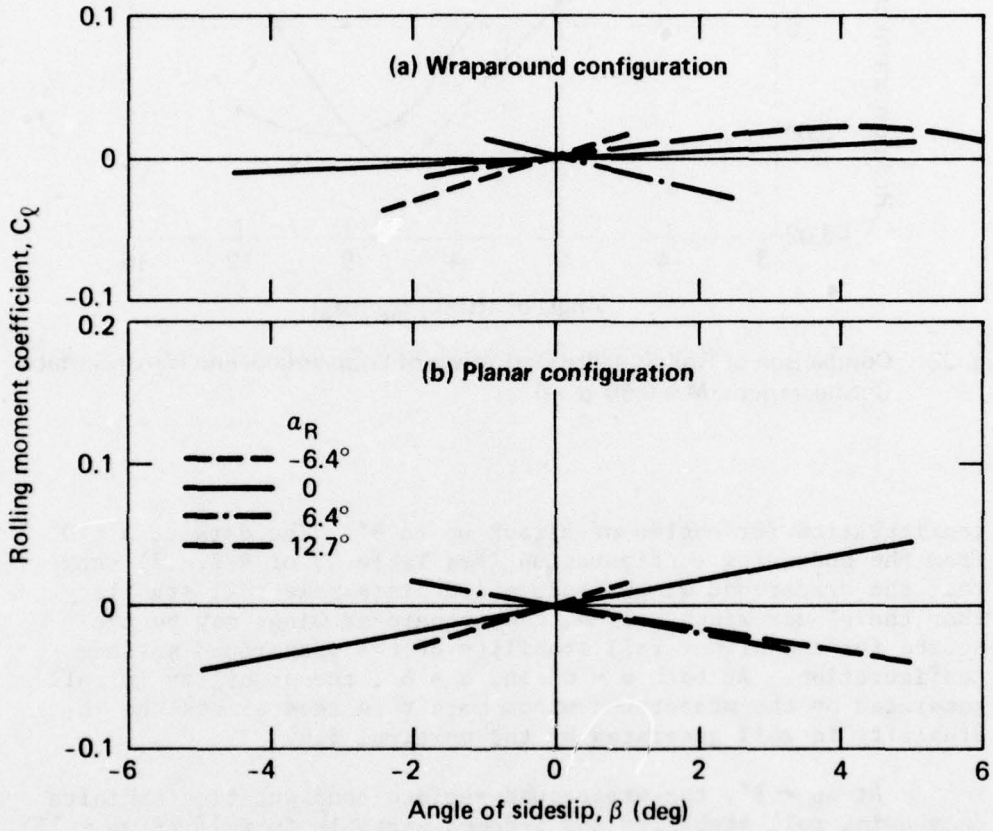

Fig. 33 Effect of Angle of Sideslip on Rolling Moment Coefficient, M = 0.80

ROLL CONTROL

The roll control effectiveness, C_{ℓ_δ}, of the wraparound tails is generally equal to or better than that of the planar tails (Fig. 34). At $\alpha > 0$, C_{ℓ_δ} decreases with increasing α for the wraparound tails but not as much as it does with the planar tails. The reduction of C_{ℓ_δ} with α is due to the onset of stall of the left panel at $\alpha_H \approx 12°$ (see Fig. 23). The importance of this reduced value of C_{ℓ_δ} (at the higher angles of attack) on aerodynamic performance depends on potential mission requirements. C_{ℓ_δ} is not very dependent on sideslip angle, β (Fig. 35).

CONTROL INTERACTIONS

Limited investigations were conducted to determine the extent of control interactions when the controls are deflected in combination. The interaction of yaw control on pitch control and *vice versa were found to be negligible* (Ref. 20). Both the induced roll resulting from yaw control and the induced yaw resulting from roll control were also investigated. The results of these investigations and an analysis of the consequences of roll-yaw control coupling are discussed next.

Rolling Moment Induced from Yaw Control

The yaw deflection produces a generally undesirable (but controllable) rolling moment that is somewhat lower for the wraparound- than for the planar-surface configuration (Fig. 36) even though the yaw control panel is planar for both configurations.

An explanation of the component contributions to $\Delta C_\ell/i_\gamma$ for the wraparound- and planar-surface configurations shows (Fig. 37) that:

1. For the planar-surface configuration, the planar wings in combination with the planar horizontal tails have very little influence on $\Delta C_\ell/i_\gamma$ for $\alpha \leq 8°$ (compare B_2V_1 data with $B_2W_pH_pV_1$ data), and

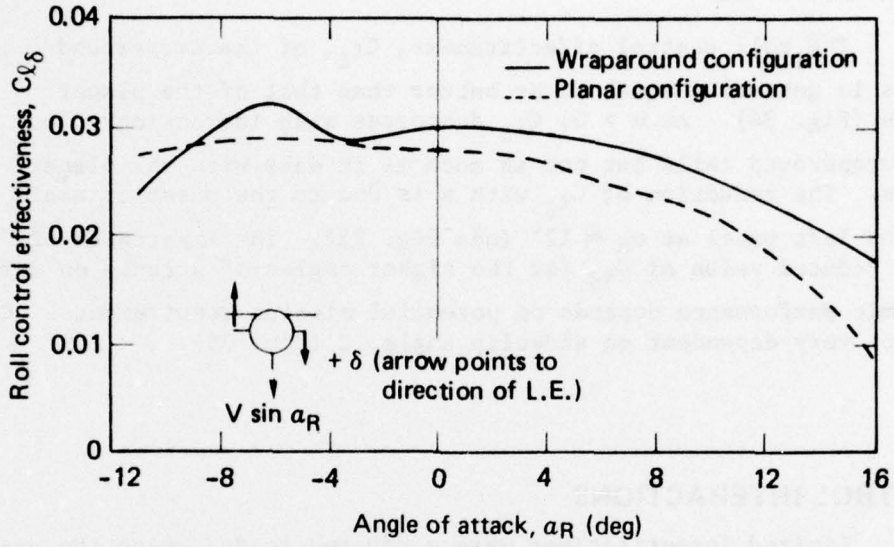

Fig. 34 Comparison of Roll Control Effectiveness of Wraparound- and Planar-Surface Configurations; M = 0.80, $\beta = 0°$

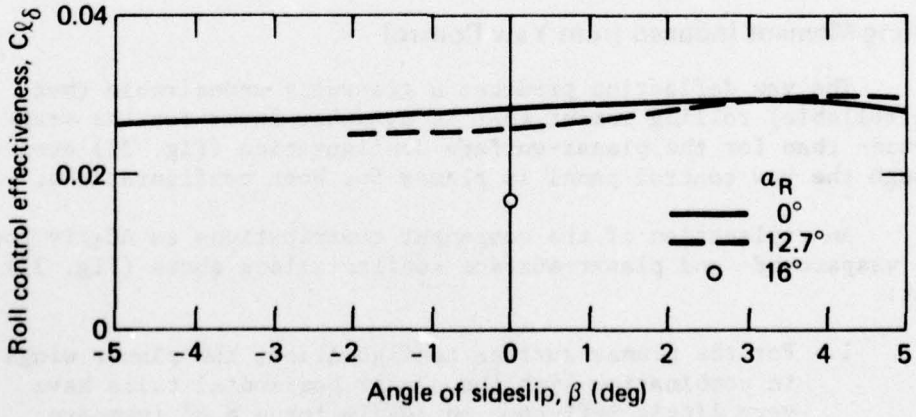

Fig. 35 Effect of Angle of Sideslip on Roll Control Effectiveness of Wraparound-Surface Configurations, M = 0.80

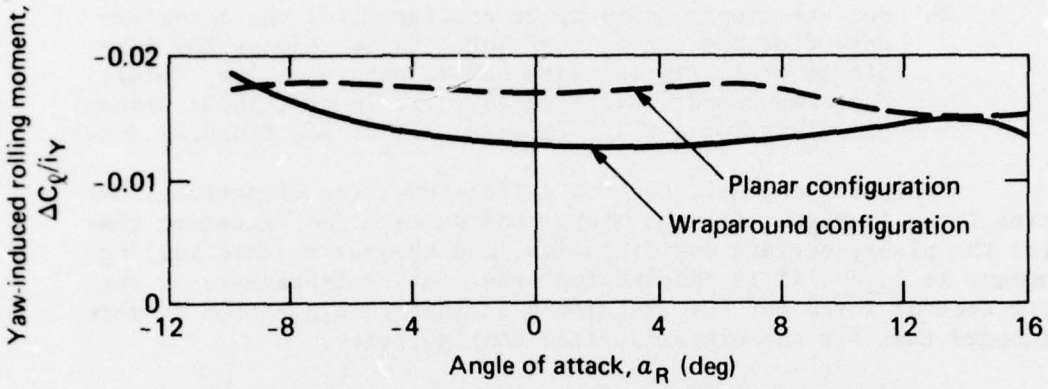

Fig. 36 Comparison of Yaw-Induced Rolling Moment of Wraparound- and Planar-Surface Configurations; M = 0.80, $\beta = 0°$

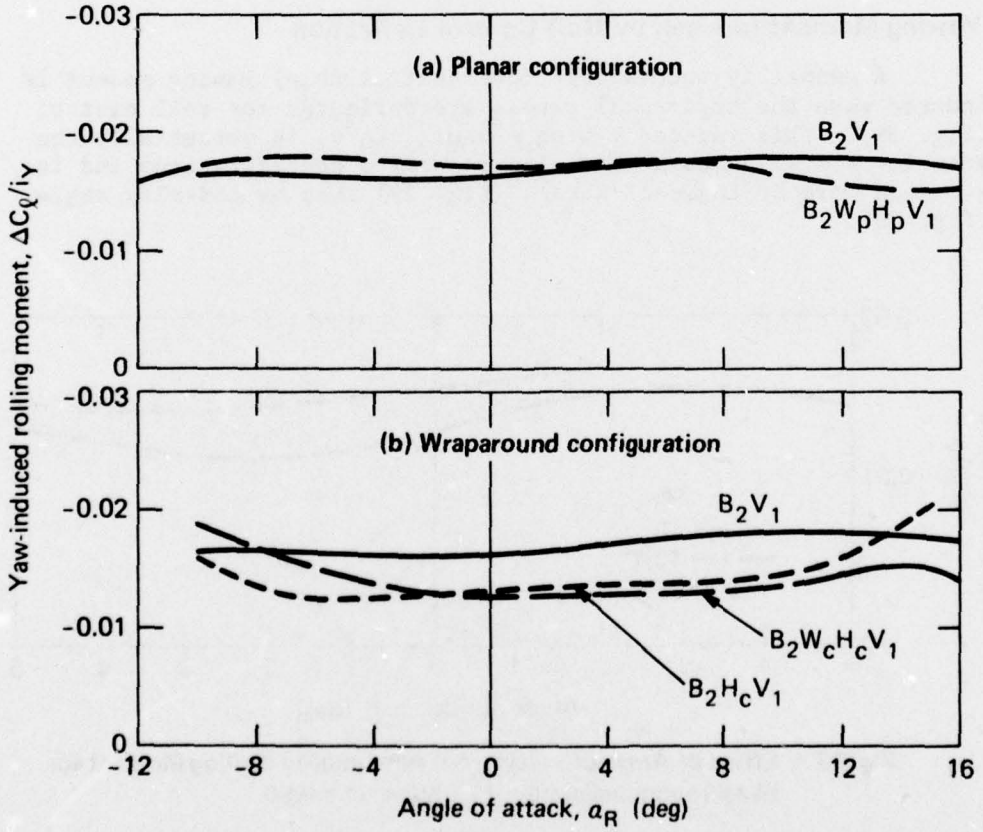

Fig. 37 Contribution of Components to Yaw-Induced Rolling Moment; M = 0.80, $\beta = 0°$

2. For the wraparound-surface configuration the interference from the curved horizontal tails reduces the magnitude of $\Delta C_\ell/i_\gamma$ (compare $B_2H_CV_1$ data with B_2V_1 data); the wraparound wings have very little additional effect on $\Delta C_\ell/i_\gamma$ for $\alpha \leq 10°$ (compare $B_2H_CV_1$ and $B_2W_CH_CV_1$ data).

Since for the same control deflections, the directional control force is higher for the wraparound-surface configuration than for the planar-surface configuration, and the yaw-induced rolling moment is lower, it is deduced that the center-of-pressure of the yaw control force for the wraparound-surface configuration is more inboard than for the planar-surface configuration.

A deflection of the horizontal tails towards the vertical panel does not change the magnitude of the yaw-induced rolling moment (Ref. 21). The sideslip angle β has only a slight effect on the yaw-induced rolling moment $\Delta C_\ell/i_\gamma$ (Fig. 38).

Yawing Moment Induced by Roll-Control Deflection

A generally undesirable (but controllable) yawing moment is induced when the horizontal panels are deflected for roll control (Fig. 39). This induced yawing moment, $\Delta C_n/\delta$, is essentially the same for the wraparound- and planar-surface configurations and is affected more by angle-of-attack (Fig. 39) than by sideslip angle (Fig. 40).

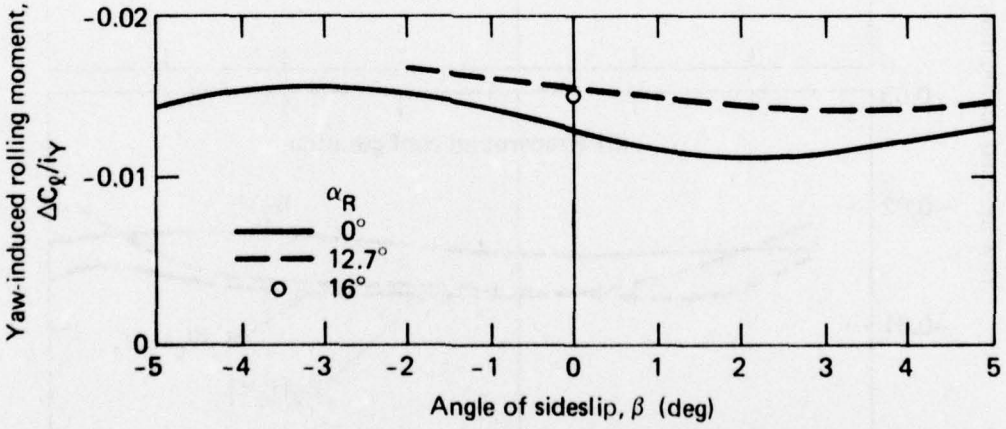

Fig. 38 Effect of Angle of Sideslip on Yaw-Induced Rolling Moment for Wraparound-Surface Configuration, M = 0.80

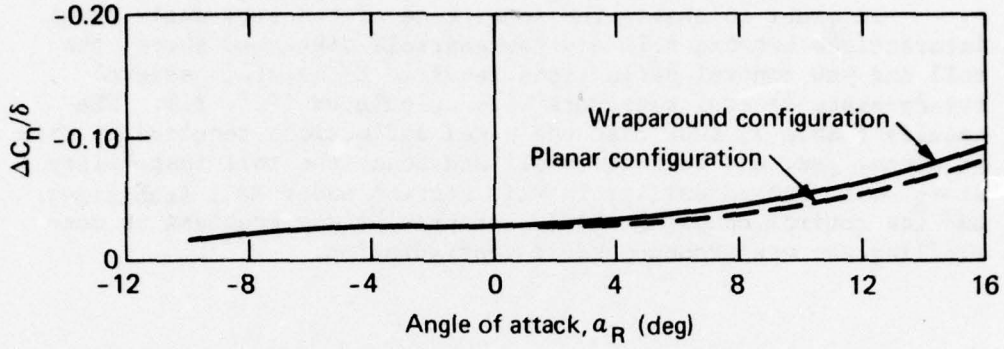

Fig. 39 Comparison of Roll-Induced Yawing Moment of Wraparound- and Planar-Surface Configurations; M = 0.80, $X_{c.g.}/\ell_B = 0.55$, $\beta = 0°$

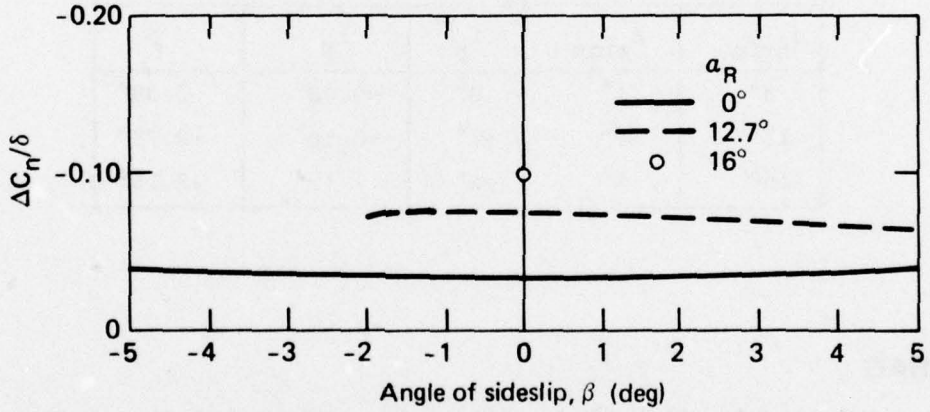

Fig. 40 Effect of Angle of Sideslip on Roll-Induced Yawing Moment of Wraparound-Surface Configuration; M = 0.80, $X_{c.g.}/\ell_B = 0.55$

Evaluation of Roll-Yaw Control Coupling

In order to assess the importance of the apparently large interactions between roll and yaw controls discussed above, the roll and yaw control deflections required to maintain several steady-state lateral maneuvers were calculated (Ref. 21). The results (Table 3) show that the panel deflections required to trim in pitch, yaw, and roll are small and hence the roll instability at $\alpha_R \gtrsim 11°$ (noted earlier in this section under Roll Stability) and the control coupling should not present any problems in controlling the wraparound-surface configuration.

Table 3

Control Surface Deflections Required to Trim at Various Steady-State Maneuvers; M = 0.80, Wraparound-Surface Configuration

Assumed Maneuver		Calculated Control Surface Deflections for Trim		
α_{trim}	β_{trim}	i_p	i_Y	δ
8°	1°	0°	-0.02°	0.38°
12°	3°	-2°	-0.16°	-0.72°
16°	5°	-4°	7.12°	-2.15°

DRAG

As previously stated, the models used in these investigations were not optimized for drag. The measurement of drag was not a primary purpose of the investigations, but drag measurements were obtained because the drag element was an integral component of the strain-gauge balance used in the test.

The drag-rise characteristics of the wraparound-surface configuration are given in Fig. 41 for Re/ft = 7.7×10^6. The drag-rise Mach number is about 0.80. (The drag-rise Mach number is defined as the Mach number at which C_{D_o} is 10% greater than the value of C_{D_o} in incompressible flow.) This Mach number, of course, can

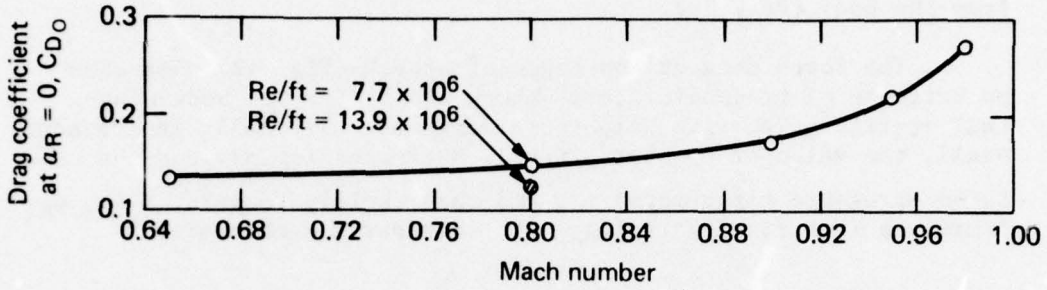

Fig. 41 Drag-Rise Characteristics of Wraparound-Surface Configuration

be increased by appropriate design for drag optimization. Other drag data obtained in these investigations are presented in Ref. 19.

MISCELLANEOUS STUDIES

Three miscellaneous studies were conducted during the tests of the wraparound-surface configuration in order to understand better the results. They are (a) low angle-of-attack transonic stall, (b) high angle-of-attack stall, and (c) effects of surface curvature on the induced roll generated by an elevated wing in pure sideslip. In addition, limited investigations were made to determine (a) the effectiveness of a wraparound vertical tail in producing directional stability, and (b) the gross aerodynamic effects of a crude body cavity at the wing location that simulates the body contour into which the wraparound wings of a tube-launched missile would be folded prior to deployment. The results of these miscellaneous studies are summarized below.

Low-α Transonic Stall

Oil-flow visualization and low angle-of-attack force studies were conducted at Mach numbers ranging from 0.65 to 0.98 at the beginning of the investigations of wraparound-surface configurations in order to select judiciously a test Mach number.

Photographs of the flow patterns over the planar wing for Mach numbers ranging from 0.65 to 0.95, and over the wraparound

wing for Mach numbers 0.80 and 0.90, show no evidence of flow separation on the wing or of any strong compressibility effects from the body (Ref. 19).

The force data at low angle-of-attack (Fig. 42) also show no evidence of transonic stall (shock stall) for the body-wing-tail configuration with wraparound surfaces. Typically in transonic stall, the value of C_{N_α} for airfoils decreases rapidly and the center-of-pressure first moves aft and then rapidly forward, i.e., C_{m_α} increases (positively) rapidly with increasing Mach number.

High-α Stall

Because there was no strong evidence of radical stall for angle-of-attack up to 16°, for the wraparound-surface configuration having a high wing and undeflected control surfaces a run was made to the highest angle-of-attack permitted by the test equipment, to determine the stall characteristics. The results show (Fig. 43) that stall occurs at $\alpha_R \approx 16.5°$, but there is only a mild effect on C_N. (Note that additional lift is available beyond the stall angle.)

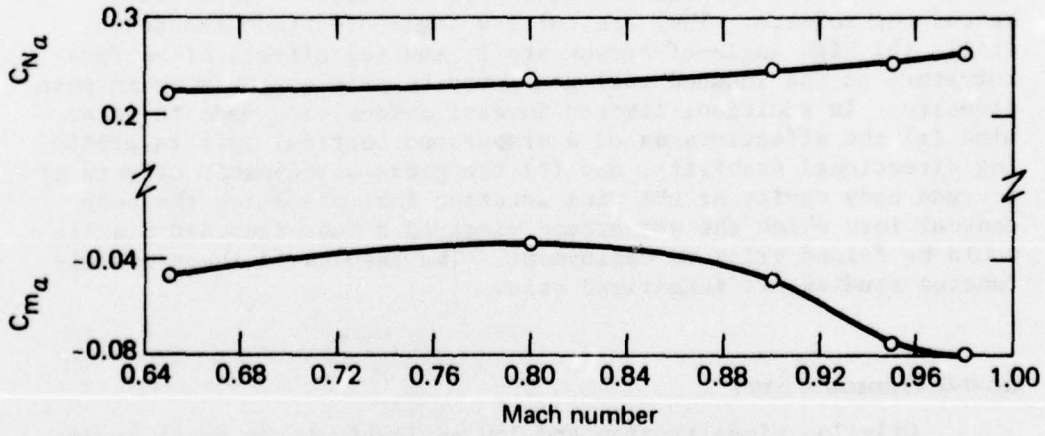

Fig. 42 Effect of Mach Number on Linearized Longitudinal Stability Characteristics of the Wraparound-Surface Configuration; $\alpha_R = 0°$, $X_{c.g.}/\ell_B = 0.55$

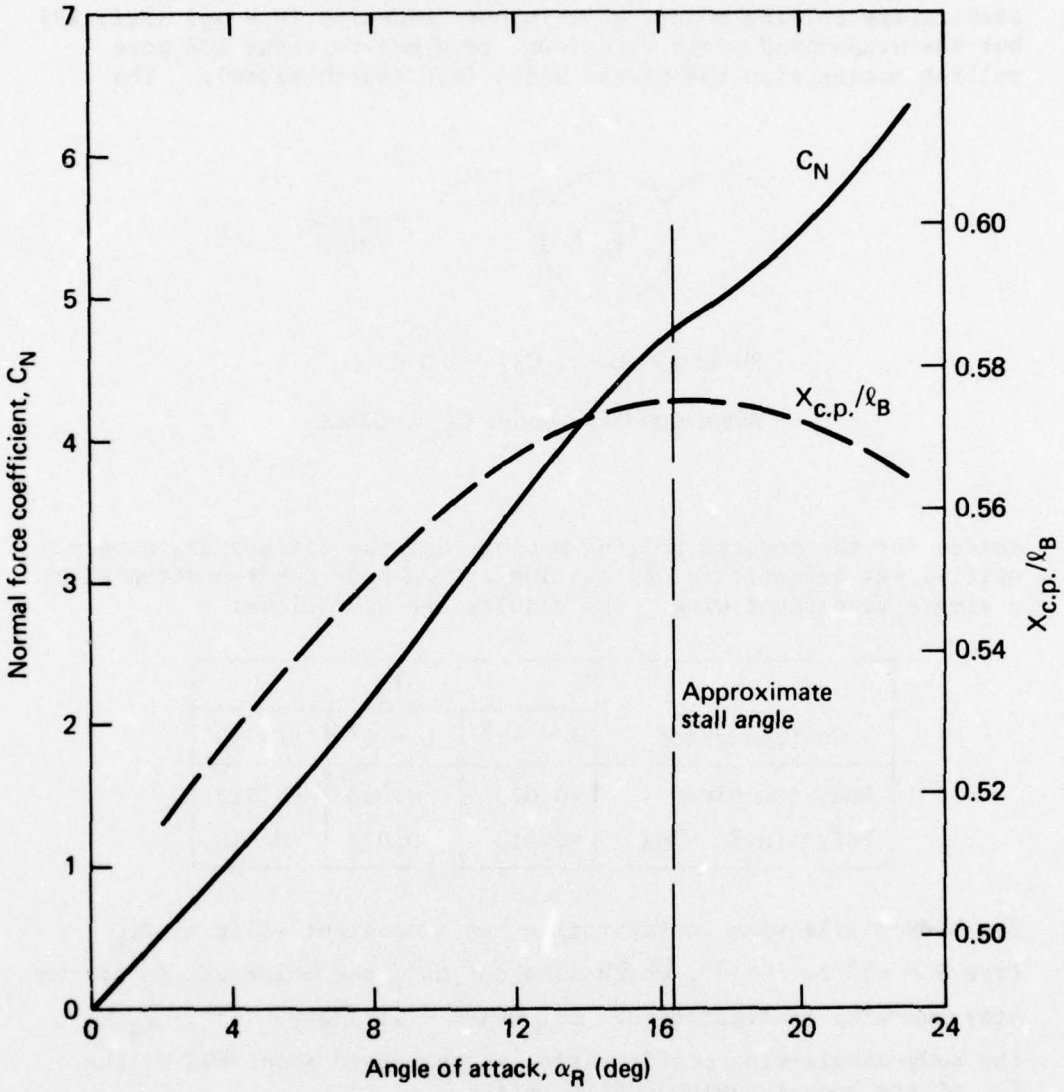

Fig. 43 Stall Characteristics of the Wraparound-Surface Configuration, M = 0.80

Induced Roll in Sideslip

Both planar and wraparound wings were found to generate a stabilizing rolling moment when in pure sideslip ($\beta = \alpha_R$) (Ref. 19), but the wraparound wings were found to generate about 50% more rolling moment than the planar wings (see sketch below). The

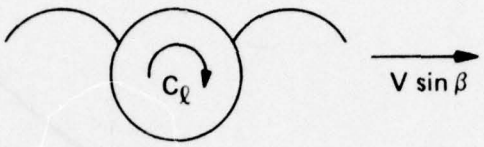

Planar wing-body: $C_{\ell_\beta} = -0.016$

Wraparound wing-body: $C_{\ell_\beta} = -0.023$

source for the induced rolling moment (not the difference, necessarily) was investigated by testing a wing-body configuration with a single wraparound wing. The results are as follows:

Configuration	C_{ℓ_β}		
	$\beta = -5°$	$\beta = 0°$	$\beta = +5°$
Body-two wings	-0.023	-0.023	-0.023
Body-single wing	-0.013	-0.013	-0.018

The body-single-wing configuration has a constant value of C_{ℓ_β} from $\beta = -5°$ to $\beta = 0°$, which is about half the value of C_{ℓ_β} of the body-two-wing configuration. Between $\beta = 0°$ and $\beta = +5°$, C_{ℓ_β} of the body-single-wing configuration increases to about 80% of the C_{ℓ_β} of the body-two-wing configuration.

From these results and observations and from the normal force data, the lateral centers-of-pressure of the roll-producing forces and the direction of these forces are deduced to be located on the body-single-wing configuration as shown in the sketches that follow:

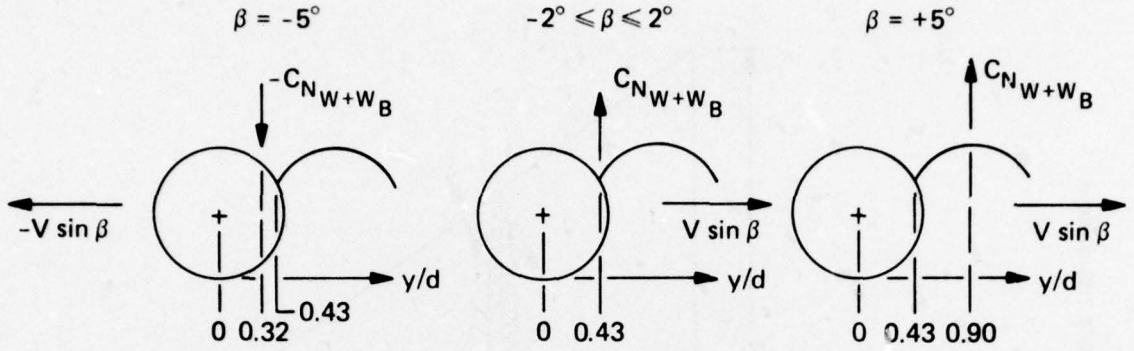

For the body-two-wing configuration a pure couple is obtained at $\beta = 0$ (i.e., $\partial C_{N_{W+W_B}}/\partial\beta = 0$, and $C_{\ell_\beta} \neq 0$) but not at $\beta \neq 0$. In longitudinal position, the center-of-pressure of the roll-producing force is at 37% of the wing root chord.

From the above sketches, it is seen that a low-wing (convex side windward at $+\alpha$) configuration would generate a destabilizing rolling moment.

The horizontal tails, which are located at the mid-plane of the body, did not produce a rolling moment when the body-tail was in pure sideslip.

Wraparound Vertical Stabilizer

All investigations of body-wing-tail configurations discussed in this report have involved planar vertical tails, thereby retaining a vertical plane of symmetry (the plane of angle-of-attack, α). Consideration was also given to the possible use of a wraparound vertical tail (Fig. 44). From the results of Ref. 19 (see Figs. 27, 28, 30, and 31 in Ref. 19), it was determined that the wraparound horizontal tails provided essentially the same normal force (and stabilizing moment in pitch) as the planar horizontal tails of the same projected planform. Thus it was surmised that a wraparound <u>vertical</u> tail might provide the same yaw force (and stabilizing moment in yaw) as the planar vertical tail of the same projected planform. A single run at $\alpha = 0$ on a configuration consisting of a body and wraparound vertical tail showed that the wraparound vertical tail provided slightly more directional stability than did the planar vertical tail (see following tabulation).

THE JOHNS HOPKINS UNIVERSITY
APPLIED PHYSICS LABORATORY
LAUREL, MARYLAND

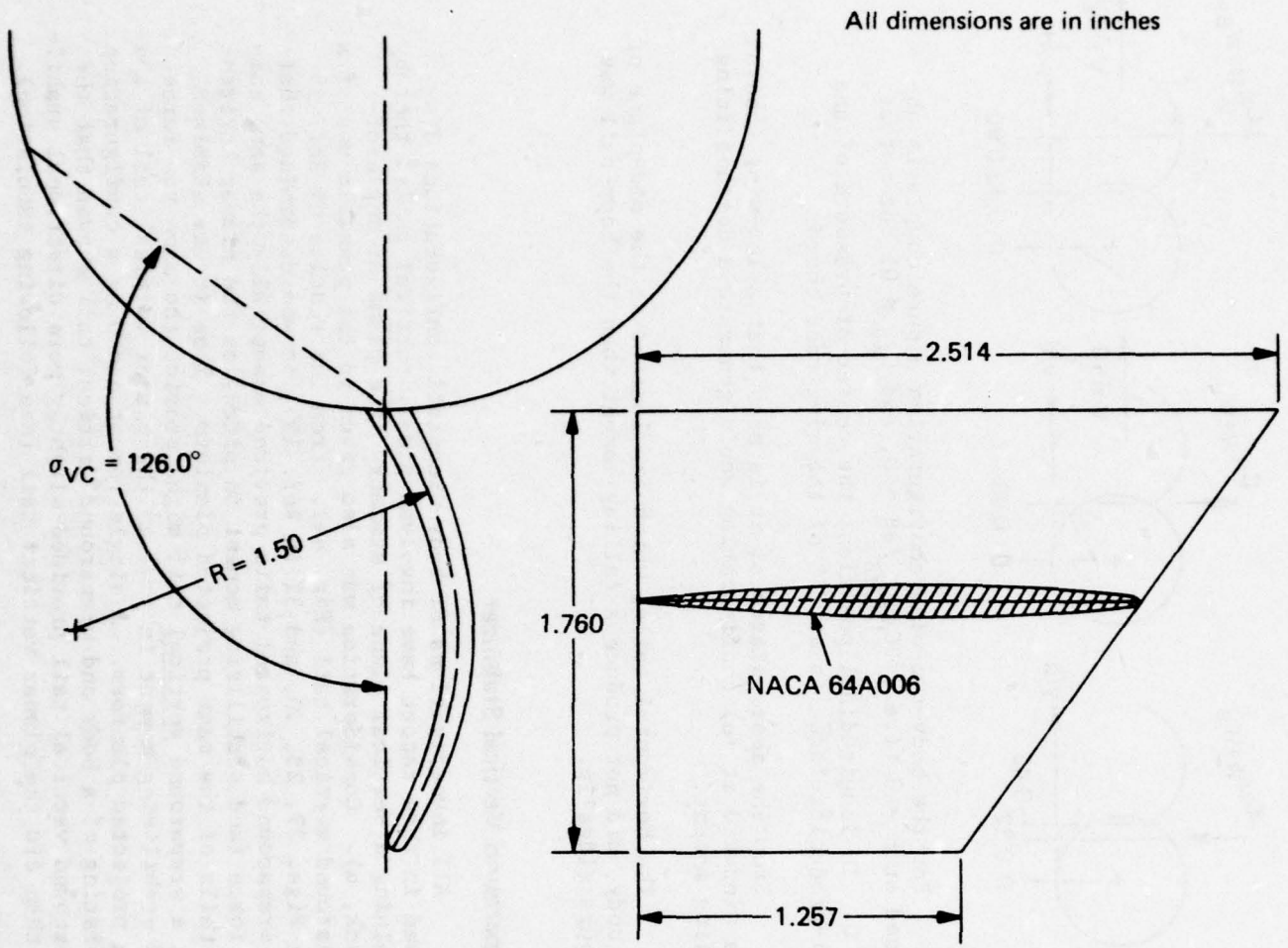

Fig. 44 Wraparound Vertical Tail (V_{CI}) Design

Configuration	C_{Y_β}	C_{n_β}	C_{ℓ_β}
B_2V_1	-0.080	0.006	0.021
B_2V_{C1}	-0.084	0.016	0.022

From these limited results and from the investigations reported throughout this report, it appears that a configuration that has all wraparound surfaces (i.e., wings, longitudinal stabilizers and controls, and directional stabilizer and control) is aerodynamically feasible.

Effects of Crude Body Cavity on Longitudinal Stability and Control

The model used in these investigations (Fig. 45) provides only a crude simulation of the cavity remaining on the wing section of the body when the wings are unfolded. Nevertheless, this crude model shows very little effect from the body cavity on longitudinal stability and control of the configuration that has the 1/4-chord point of the wing M.A.C. located at 50% of the body length (Fig. 46). Similarly, component data showed little effect on C_N and C_m from the body cavity (Ref. 25). It is expected, therefore, that a well-designed body contour that reduced drag would not affect lift and hence would increase the lift-to-drag ratio.

Ref. 25. E. F. Lucero, "Experimental Results at Mach 0.80 of the Effect of Body Cavity on the Longitudinal Stability and Control Characteristics of the Wrap-Around Surface Project (WASP) Configuration," APL/JHU BFD-1-75-012, 9 June 1975.

Fig. 45 Wraparound-Surface Model with Filleted Body Cavity

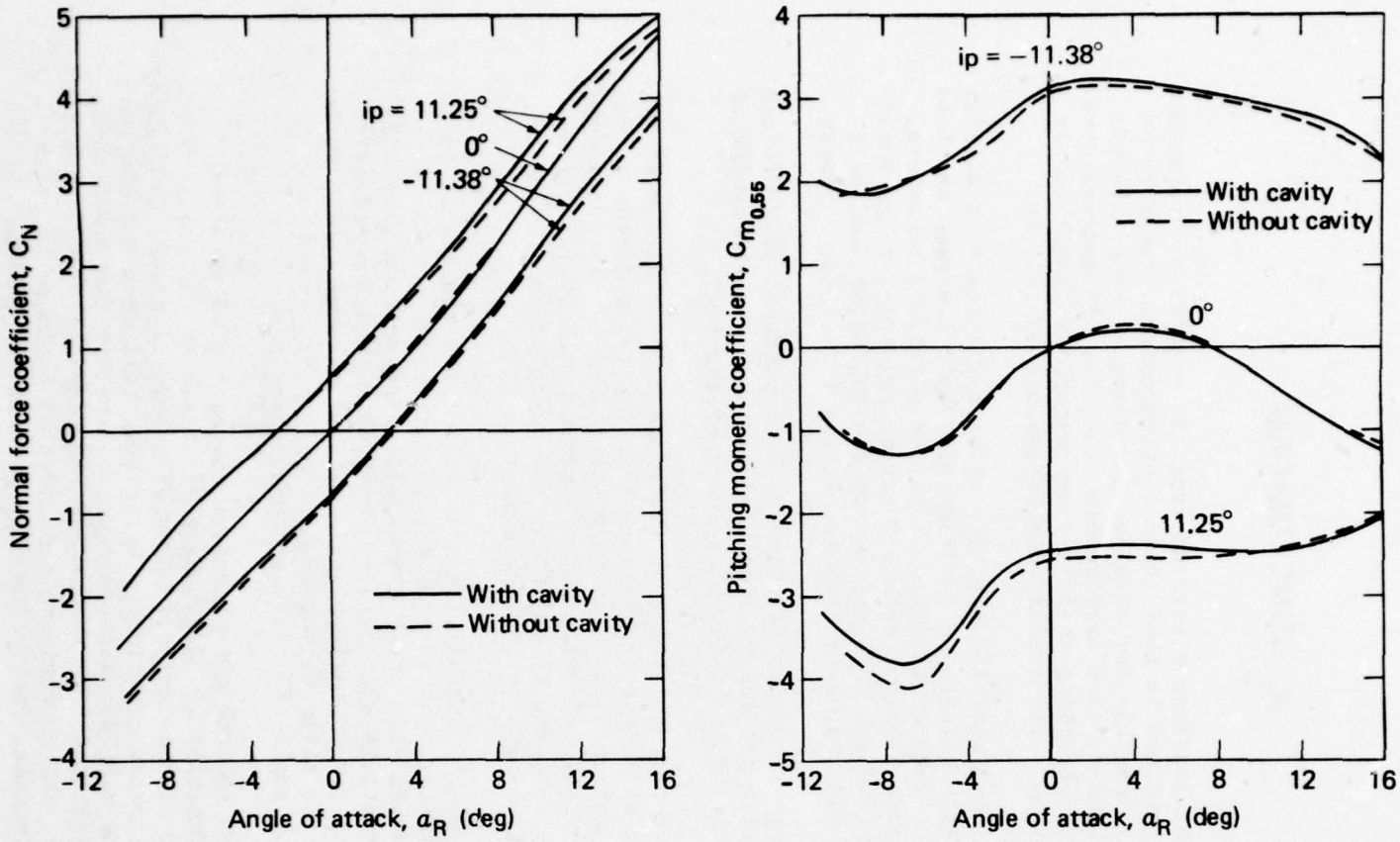

Fig. 46 Effect of Body Cavity on Normal Force and Pitching Moment Coefficients for Wraparound-Surface Configuration, M = 0.80

4. CONCLUSIONS

A general conclusion derived from the studies of wraparound-surface configurations is that these configurations appear to be aerodynamically feasible for missiles traveling at high subsonic speeds, using bank-to-turn aerodynamic controls. No unusual aerodynamic behavior affecting stability or control was exhibited by the configurations. Particular conclusions are as follows:

1. The longitudinal stability characteristics of a missile configuration with wraparound surfaces are about the same as those using planar surfaces of the same projected planform; therefore, the force and moment characteristics can be predicted to an accuracy that is sufficient for preliminary design, using available predictive methods that have been formulated for planar surfaces.

2. A high wing with its concave side windward is preferred to a low wing with its convex side windward from the standpoint of lift of the wing and stability efficiency of the tail.

3. The horizontal tails of the wraparound-surface configuration are more efficient stabilizers than the tails of the planar-surface configuration. The stability efficiency of the wraparound tails is under-predicted using planar-surface methods. The predictions can be improved by adjusting the calculations, using an "effective" tail height as suggested in this study.

4. The pitch control effectiveness of the wraparound tails is generally greater than that of the planar tails when the controls are deflected with their convex side windward and generally less when the controls are deflected with their concave side windward; therefore, for a stable missile with wraparound tails, it is preferred that the tails be mounted so that their concave side is windward when at angle-of-attack and when undeflected.

The pitch control effectiveness correlates as an almost single-valued function of local angle-of-attack at the tail. Therefore, the pitch control effectiveness of a body-wing-tail configuration can be estimated empirically using body-tail data and the calculated value of wing downwash as described herein for wraparound-surface configurations. In the absence of body-tail data, theoretical predictions, which provide a conservative estimate of pitch control effectiveness, can be used for preliminary design.

5. The wraparound-surface configuration has directional stability characteristics that are generally more favorable than those of the planar-surface configuration. A windward vertical panel for directional stability is more efficient than a leeward panel, but is equally efficient for directional control.

6. The roll control effectiveness of the wraparound tails is equal to or better than that of the planar tails.

7. Less than $|5°|$ pitch control deflection is required to trim the wraparound-surface configuration in pitch-plane maneuvers for angles-of-attack up to 16°. For combined pitch-yaw-roll maneuvers where control coupling is observed, less than 2.2° in roll control deflection and less than 7.2° in yaw control deflection are required to trim.

8. The high-wing-body configurations generate stabilizing rolling moments when in pure sideslip. The wraparound wings generate about twice as much rolling moment as the planar wings.

9. A wraparound vertical stabilizer produces more directional stability than, and about the same roll stability as, the planar vertical stabilizer. An "all"-wraparound-surface configuration appears to be aerodynamically feasible.

10. The longitudinal stability and control characteristics of the wraparound-surface configuration are not expected to be affected by the cavity remaining on the body when the wings are deployed from their folded position.

5. RECOMMENDATIONS

POSSIBLE IMPROVEMENTS

The wraparound-surface configuration investigated in these studies was not optimized for lift or drag, in order to keep the configuration simple and the cost minimal. The lift characteristics could be improved by using a cambered profile for the wing and possibly a super-critical profile, depending on the cruise-speed requirements. An improvement in design for drag optimization would include a proper nose design; body contouring not only to accommodate the wing when folded in its stowed position, but also to reduce drag at high subsonic speeds; boattailing; wing planform shaping; and a super-critical wing profile for operation at transonic speed.

FUTURE WORK

The airloading characteristics of wraparound-surfaces during post-launch unfolding has not been determined experimentally for any speed regime. This information would be needed for the design of the panel structure and erection mechanism.

It is recommended that the aerodynamic loading during unfolding of wraparound surfaces be investigated in the wind tunnel.

ACKNOWLEDGMENT

The work described in this report was performed under the sponsorship of the Materials and Mechanics Division, Naval Sea Systems Command. Mr. L. Pasiuk, NAVSEA-0351, was the Problem Sponsor. The contributions of Dr. L. L. Cronvich and Mr. E. T. Marley are appreciated. Thanks are due to Mrs. Helen Tate for typing the original manuscript and all previous reports pertinent to this study.

REFERENCES

1. H. J. Gauzza, "Static Stability Test of Tangent and Wrap-Around Fin Configurations at Supersonic Speeds," NAVORD Report 3743, 17 January 1955.

2. R. Franklin Wells, "Investigation of the Aerodynamic Characteristics of a Model of a Rocket Missile with Several Arrangements of Folding Fins at Mach Numbers of 1.75, 2.15, 2.48, and 2.87," NASA TMX-234, April 1960.

3. H. A. Featherstone, "The Aerodynamic Characteristics of Curved Tail Fins," General Dynamics/Pomona GDC-ERR-PO-019, September 1960.

4. F. J. Regan and V. L. Schermerhorn, "Supersonic Magnus Measurements of the 10-Caliber Army-Navy Spinner Projectile with Wrap-Around Fins," NOL TR 70-211, 1 October 1970.

5. Proceedings of the Ninth Meeting of the Exterior Ballistics Panel 0-7, Vol. II, Session I, *Weapon Aerodynamics*, DREV M-2184172, September to October 1971 (see Bibliography for pertinent papers).

6. J. C. Craft and J. Skorupski, "Static Aerodynamic Stability Characteristics of Munitions Designs at Transonic Mach Numbers," USAMC Tech Report RD-73-3, February 1973.

7. C. W. Dahlke and J. C. Craft, "Aerodynamic Characteristics of Wrap Around Fins Mounted on Bodies of Revolution, and Their Influence on Missile Static Stability at Mach Numbers from 0.3 to 1.3," USAMC RD-TM-72-1, Vol. I, March 1972, Vol. II, April 1972.

8. E. F. Lucero, "Proposal for Aerodynamic Investigation of Transonic Missile Configurations Incorporating Wrap-Around Lifting Surfaces, Part I: Aerodynamic Configuration Design," APL/JHU BBA-2-73-001, 2 April 1973.

9. F. W. Diederich, "A Planform Parameter for Correlating Certain Aerodynamic Characteristics of Swept Wings," NACA TN 2335, April 1951.

10. W. C. Pitts, J. N. Nielsen, and G. E. Kaattari, "Lift and Center-of-Pressure of Wing-Body-Tail Combinations at Subsonic, Transonic, and Supersonic Speeds," NACA Report 1307, 1957.

11. J. L. Decker, "Prediction of Downwash at Various Angles of Attack for Arbitrary Tail Locations," Aeronaut, Eng. Rev., Vol. 15, August 1956.

12. "USAF Stability and Control DATCOM," McDonnell-Douglas Corp., Douglas Aircraft Division, under Contract to Air Force Flight Dynamics Laboratory, Wright-Patterson Air Force Base, Ohio, October 1960.

13. E. F. Lucero, "Test Operations Report, WASP Wind Tunnel Test No. HST 361-0 (August 7 - August 10, 1973)," APL/JHU BBA-2-73-005, 31 August 1973.

14. E. F. Lucero, "Test Operations Report for WASP Controls Test GD/Convair HST 361-1 (August 21 - August 24, 1974)," APL/JHU BFD-1-74-022, 19 September 1974.

15. "International Aerospace, 1972 Specification Tables" (Reprinted from Aviat. Week Space Technol.), 13 March 1972.

16. B. N. Daley and R. S. Dick, "Effect of Thickness Camber and Thickness Distribution on Airfoil Characteristics at Mach Numbers up to 1.0," NACA TN 3607, March 1956.

17. E. C. Allen, "Experimental Investigations of the Effects of Planform Taper on the Aerodynamic Characteristics of Symmetrical Unswept Wings of Varying Aspect Ratio," NACA RM A53 C19, 29 May 1953.

18. E. F. Lucero and J. J. Pasierb, "Short Course on Current Transonic Flow Problems — Theories and Applications," APL/JHU BBA-0-74-003, 1 February 1974.

19. E. F. Lucero, "Experimental Results of High Subsonic Aerodynamic Longitudinal Stability Characteristics of Bank-to-Turn Configurations Incorporating Wrap-Around Surfaces with Subsonic Sections," APL/JHU BFD-1-74-009, 12 February 1975.

20. E. F. Lucero, "Experimental Study at M = 0.8 of the Aerodynamic Controllability of the Missile Configuration for the Wrap-Around Surface Project (WASP)," APL/JHU BFD-1-75-006, 8 May 1975.

21. E. F. Lucero, "Wrap-Around Surface Project (WASP) Studies — Analysis of Experimental Data on Lateral Stability and on Effects of Sideslip on Yaw and Roll Control, M = 0.8," APL/JHU BFD-1-75-010, 30 May 1975.

22. E. C. Polhamus, "Effect of Nose Shape on Subsonic Aerodynamic Characteristics of a Body of Revolution Having a Fineness Ratio of 10.94," NACA RM L57 F25, 12 August 1957.

23. Handbook of Supersonic Aerodynamics, Bodies of Revolution, NAVWEPS Report 1488 (Vol. 3, Sect. 8), October 1961.

24. E. C. Polhamus, "Predictions of Vortex-Lift Characteristics by a Leading Edge Suction Analogy," J. Aircr., Vol. 8, No. 4, April 1971.

25. E. F. Lucero, "Experimental Results at Mach 0.80 of the Effect of Body Cavity on the Longitudinal Stability and Control Characteristics of the Wrap-Around Surface Project (WASP) Configuration," APL/JHU BFD-1-75-012, 9 June 1975.

BIBLIOGRAPHY (Listed Chronologically)

1. J. D. Nicolaides, C. W. Ingram, J. M. Martin, and A. M. Morrison, "Nonlinear Aerodynamics Stability Characteristics of the 2.75 Wrap-Around Fin Configuration," Paper No. 31, Proceedings of the 8th Navy Symposium on Aeroballistics, Vol. 3, 6-8 May 1969.

2. T. A. Mottinger and W. D. Washington, "An Experimental Investigation of Low Aspect Ratio Fins Tested at Transonic Speeds on a Reflection Plane," USAMC RD-TM-71-15, July 1971.

3. R. A. Deep, "Static Aerodynamic Characteristics of WAF at Transonic Speeds," Paper I-2, Proceedings of the 9th Meeting of the Exterior Ballistics Panel 0-7, Vol. II, Session I: Weapon Aerodynamics, DREV M-2184/72, September-October 1971.

4. J. E. Holmes and S. M. Hastings, "TTCP Panel 0-7 Standard Wrap-Around Fin Supersonic Pressure Distributions," Paper I-3, Proceedings of the 9th Meeting of the Exterior Ballistics Panel 0-7, Vol. II, Session I: Weapon Aerodynamics, DREV M-2184/72, September-October 1971.

5. R. C. Dixon and M. Laviolette, "A Summary of Results from a Joint DREV/NAE Wind Tunnel Programme on WAF Stabilized Model," Paper I-4, Proceedings of the 9th Meeting of the Exterior Ballistics Panel 0-7, Vol. II, Session I: Weapon Aerodynamics, DREV M-2184/72, September-October 1971.

6. B. L. Carrington, C. V. Hurdle, and R. K. Faucett, "Wrap-Around Fins — The Results of a Subsonic Parametric Study," Paper I-5, Proceedings of the 9th Meeting of the Exterior Ballistics Panel 0-7, Vol. II, Session I: Weapon Aerodynamics, DREV M-2184/72, September-October 1971.

7. Wrap-Around Fin Bibliography, Paper I-6, Proceedings of the 9th Meeting of the Exterior Ballistics Panel 0-7, Vol. II, Session I: Weapon Aerodynamics, DREV M-2184/72, September-October 1971.

8. C. W. Dahlke, "Experimental Investigation of Several Wrap-Around Fins on Bodies of Revolution from Mach 0.3 to 1.3," USAMC RD-TM-71-12, September 1971.

9. M. L. Robinson and C. E. Fenton, "Static Aerodynamic Characteristics of a Wrap-Around Fin Configuration with Small Rolling Moments at Low Incidence," Australian Defense Scientific Service, WRE-TN-527 (WR&D), November 1971.

10. C. W. Dahlke and J. C. Craft, "Static Aerodynamic Stability Characteristics of a Body of Revolution with Wrap-Around Fins at Mach Numbers from 0.5 to 1.3," USAMC RD-TM-72-6, June 1972.

11. C. W. Dahlke and J. C. Craft, "Static Aerodynamic Stability Characteristics of Bodies of Revolution with Wrap-Around Fins at Mach Numbers from 1.6 to 2.86," USAMC RD-TM-72-14, September 1972.

12. J. S. Wingrove, R. G. Williams, and T. W. F. Moore, "An Analysis of the TTCP Panel (O-7) Wind Tunnel Test Programme on Configurations Employing Wrap-Around Curved Fins," B.A.C., G. W. Div. Bristol, ST. 9254, May 1973 (DDC AD 911-979L).

13. K. R. Crowell and C. T. Crowe, "Prediction of the Lift and Moment on a Slender Cylinder-Segment Wing-Body Combination," Aeronaut. J., June 1973, pp. 295-298.

14. J. E. Holmes, "Wrap-Around Fin (WAF) Pressure Distribution," NOL TR 73-107, 1 October 1973.

15. F. L. Stevens, "Analysis of the Linear Pitching and Yawing Motion of Curved-Finned Missiles," U.S. Naval Weapons Laboratory, Technical Report TR-2989, October 1973.

16. D. E. Swanson and C. T. Crowe, "Cylindrical Wing-Body Configurations for Space-Limited Applications," J. Spacecr. Rockets, Vol. 11, No. 1, January 1974.

17. F. L. Stevens, T. J. On, and T. A. Clare, "Wrap-Around vs. Cruciform Fins: Effects on Rocket Flight Performance," AIAA Paper No. 74-777, AIAA Mechanics and Control of Flight Conference, 5-9 August 1974.

18. E. F. Lucero, "Estimates of WASP Wing Loads as a Function of Wing Opening Angle," APL/JHU BFD-1-74-019, 19 July 1974.

19. E. F. Lucero, "Use of the Leading Edge Suction Analogy to Predict Wing Lift on Non-Sharp, Non-Fully Tapered Wings," APL/JHU BFD-1-75-001, 27 January 1975.

20. E. F. Lucero, "Subsonic Stability and Control Characteristics of Configurations Incorporating Wrap-Around Surfaces," J. Spacecr. Rockets, Vol. 13, No. 12, December 1976.

SYMBOLS AND NOMENCLATURE

Symbol	Definition	Dimensions
General		
A.R.	Aspect ratio of one exposed wing (tail) panel (span squared)/planform area	
c	Local chord	inches
C_D	Drag coefficient, D/qS	
C_{D_o}	C_D at $\alpha_R = 0$	
C_ℓ	Rolling moment coefficient, ℓ/qSd	
$C_{m_{0.55}}$	Pitching moment coefficient, m/qSd, about $X/\ell_B = 0.55$	
$C_{n_{0.55}}$	Yawing moment coefficient, n/qSd, about $X/\ell_B = 0.55$	
C_N	Normal force coefficient, N/qS	
C_Y	Yaw force coefficient, Y/qS	
d	Body diameter, 3.0 inches	inches
D	Drag force (see Fig. 6)	pounds
$h_{t(eff)}$	Effective tail height for wraparound surfaces (see Fig. 22)	inches
i_p	Pitch control-surface deflection (see Fig. 7)	degrees
i_Y	Yaw (directional) control-surface deflection (see Fig. 7)	degrees
ℓ	Rolling moment (see Fig. 6)	in.-lb
ℓ_B	Body length, 30 inches	inches
m	Pitching moment about $X/\ell_B = 0.55$ (see Fig. 6)	in.-lb

M	Mach number	
M.A.C.	Mean aerodynamic chord, chord at the lateral distance $\bar{y}$	inches
n	Yawing moment about $X/\ell_B = 0.55$ (see Fig. 6)	in.-lb
N	Normal force (see Fig. 6)	pounds
q_ℓ, q	Local and freestream dynamic pressure, respectively	lb/in^2
R	Body radius, R = 1.50 inches	inches
Re	Reynolds number, $Re = \frac{V\ell_B}{\nu}$	
S	Reference area, $S = \frac{\pi d^2}{4} = 7.07\ in^2$	in^2
u,v,w	Components of $\vec{V}$ (see Fig. 6)	ft/s
V	Magnitude of velocity ($\vec{V}$ is velocity vector shown in Fig. 6)	ft/s
x,y,z	Body-fixed axes (see Fig. 6)	
X	Body longitudinal station, measured rearward from nose tip	inches
$X_{c.g.}$	Center-of-gravity station	inches
$X_{c.p.}$	Longitudinal center-of-pressure station	inches
$\bar{y}$	Lateral distance of wing (tail) centroid measured from root chord parallel to the y-axis (see Figs. 2 and 1)	inches
Y	Yaw force (see Fig. 6)	pounds
Z_w	Height of projected span of wing measured vertically from the x-y plane, $Z_w = (d/2) \tan \theta_w$	inches
ΔC_F	Increment in C_F, where F = ℓ, m, n, N, or Y, resulting from the deflection of control surfaces	
C_{F_α}	$\partial C_F/\partial\alpha$ at $\alpha = 0$, where F = m, N	per degree

C_{F_β}	$\partial C_F/\partial\beta$ at $\beta = 0$, where F = ℓ, n, Y	per degree
C_{ℓ_δ}	Roll control effectiveness obtained from $\Delta C_\ell/\delta$	per degree
α	Local angle of attack (see Fig. 6)	degrees
α_H	Local angle of attack at the 1/4-chord point of the M.A.C. of the horizontal tail	degrees
α_R	Resultant angle of attack (see Fig. 6) $\alpha_R \equiv \alpha$ at $\beta = 0$; unless otherwise specified, $\alpha \equiv \alpha_R$	degrees
β	Angle of sideslip (see Fig. 6)	degrees
δ	Average differential tail deflection (see Fig. 7)	degrees
$\bar{\epsilon}$	Average downwash angle at the 1/4-chord point of the M.A.C. of the horizontal tail, $\bar{\epsilon}$ is positive in direction of $-\alpha$	degrees
η_{HV}	Tail efficiency in providing longitudinal stability $\eta_{HV} \equiv \dfrac{C_{m_{BWHV}} - C_{m_{BW}}}{C_{m_{BHV}} - C_{m_B}}$	
ν	Kinematic viscosity	ft^2/s
$\theta_W(\theta_V)$	Elevation angle of wing (vertical tail) (see Figs. 1 and 2)	degrees
$\sigma_W, \sigma_H, \sigma_{VC}$	Opening angle of wing, horizontal tail, and wraparound vertical tail, respectively (see Figs. 2 , 3, and 44)	degrees
ϕ	Aerodynamic roll angle (see Fig. 6)	degrees
$d\bar{\epsilon}/d\alpha$	Change in $\bar{\epsilon}$ with α	

Subscripts used to identify configurational components for which coefficients are given (e.g., $C_{N_{BW}}$ = normal force coefficient for body-wing configuration)

B	Body alone
BW	Body-wing
BH	Body-horizontal tail
BV	Body-vertical tail
BHV	Body-horizontal tail - vertical tail
BWHV	Body-wing-tail (full configuration)
W, W_B, B_W	Wing, wing due to body, and body due to wing, respectively, used in $C_{N_{W+W_B+B_W}} = C_{N_{BW}} - C_{N_B}$

Nomenclature of Model Parts

B	Body alone consisting of a von Karman nose* of fineness ratio 2.1 followed by a cylindrical afterbody of fineness ratio 7.9 (see Fig. 1)
B_1	Subscript "1" is used when the wing is positioned with its 1/4-chord point of the M.A.C. at 60% of the body length
B_2	Subscript "2" is used when the wing is positioned with its 1/4-chord point of the M.A.C. at 50% of the body length
H_C	Wraparound horizontal tail, concave to windward at $+\alpha$, $i_p = 0$ (see Fig. 3)

*A von Karman nose has the following geometry:

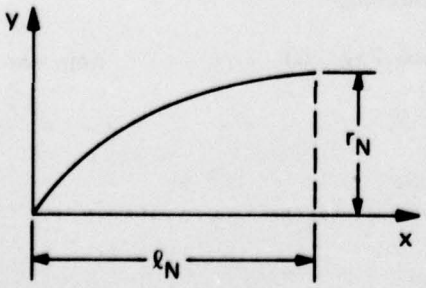

$$\frac{y}{r_N} = \sqrt{\frac{\rho - 1/2 \sin 2\rho}{\pi}},$$

where $\rho \equiv \cos^{-1}\left(1 - \frac{2x}{\ell_N}\right)$.

H_P	Planar horizontal tail
W_C	Wraparound wing, concave to inboard at $+\alpha$ (see Fig. 2)
W_P	Planar wing
V_1	Planar vertical tail
V_{C1}	Wraparound vertical tail (see Fig. 44)

INITIAL DISTRIBUTION EXTERNAL TO THE APPLIED PHYSICS LABORATORY*

The work reported in TG 1312 was done under Navy Contract N00017-72-C-4401. This work is related to Task A31 which is supported by Naval Sea Systems Command.

ORGANIZATION	LOCATION	ATTENTION	No. of Copies
DEPARTMENT OF DEFENSE			
DDC	Alexandria, VA		12
Department of the Navy			
Headquarters			
NAVSEASYSCOM	Washington, DC	SEA-035	1
		SEA-0351 (L. Pasiuk)	2
		SEA-09G3	1
NAVAIRSYSCOM	Washington, DC	AIR-320C (W. C. Volz)	1
		AIR-53012B (T. F. Martin)	1
		AIR-5524A (W. D. Greenless)	1
		AIR-50174	1
NAVPRO	Laurel, MD		1
Centers			
David W. Taylor NSRDC	Washington, DC	Dr. S. de los Santos	1
		R. M. Hartley	1
		G. S. Pick	1
		Librarian	1
NADC	Warminster, PA	Alvin Spector	1
NSWC	White Oak, MD	A. J. Goreclad	1
		S. M. Hastings	1
		J. E. Holmes	1
		F. J. Regan	1
		R. E. Wilson	1
		A. E. Winkelman	1
		Librarian	1
NSWC	Dahlgren, VA	T. A. Clare	1
		F. L. Stevens	1
		Librarian	1
NWC	China Lake, CA	S. K. Carter	1
		W. H. Clark	1
		Librarian	1
Pacific Missile Test Center	Point Mugu, CA	K. A. Larsen	1
		Librarian	1
ONR	Arlington, VA	D. W. Siegel	1
		Librarian	1
Department of the Air Force			
AFFDL	Wright Patterson AFB, Dayton, OH	E. Fleeman	1
		R. E. Nelson	1
		Librarian	1
Department of the Army			
USAMC, Redstone Arsenal	Huntsville, AL	J. C. Craft	1
		C. W. Dahlke	1
		R. Deep	1
		J. Skorupski	1
		Librarian	1
U.S. GOVERNMENT AGENCIES			
Library of Congress	Washington, DC	Librarian	1

Requests for copies of this report from DoD activities and contractors should be directed to DDC, Cameron Station, Alexandria, Virginia 22314 using DDC Form 1 and, if necessary, DDC Form 55.

*Initial distribution of this document within the Applied Physics Laboratory has been made in accordance with a list on file in the APL Technical Publications Group.

INITIAL DISTRIBUTION EXTERNAL TO THE APPLIED PHYSICS LABORATORY*

TG 1312

ORGANIZATION	LOCATION	ATTENTION	No. of Copies
National Aero. and Space Admin.			
Ames Research Center	Moffett Field, CA	G. Chapman	1
		Librarian	1
Langley Research Center	Hampton, VA	C. M. Jackson	1
		E. C. Polhamus	1
		W. C. Sawyer	1
		L. Spearman	1
		Librarian	1
UNIVERSITIES			
Washington State Univ.	Pullman, WA	C. T. Crowe	1
Auburn University	Auburn, AL	J. E. Burkhalter	1
		J. O. Nichols	1
		R. G. Pitts	1
CONTRACTORS			
General Dynamics/Convair Aero. Div.	San Diego, CA	D. Cumming	1
General Dynamics/Pomona Div.	Pomona, CA	F. C. Thomas	1
Honeywell, Inc.	Minneapolis, MN	S. Sopczak	1
Hughes Aircraft Corp., Missile Systems Div	Canoga Park, CA	J. B. Harrisberger	1
Martin Marietta Corp.	Orlando, FL	G. F. Aiello	1
McDonnall Douglas East	St. Louis, MO	R. C. Brown	1
McDonnell Douglas West	Huntington Beach, CA	M. Briggs	1
NEAR, Inc.	Mountain View, CA	J. Nielsen	1
		J. Fidler	1
Raytheon Corp.	Bedford, MA	D. P. Forsmo	1
Rockwell Int'l/Missiles Sys. Div.	Columbus, OH	J. E. Rachner	1
Sanders Assoc. Inc.	Nashua, NH	J. Smith	1

*Initial distribution of this document within the Applied Physics Laboratory has been made in accordance with a list on file in the APL Technical Publications Group.